

From OCR and ECAR to energy: Perspectives on the design and interpretation of bioenergetics studies

Received for publication, January 11, 2021, and in revised form, August 25, 2021. Published, Papers in Press, August 28, 2021, <https://doi.org/10.1016/j.jbc.2021.101140>

Cameron A. Schmidt^{1,2}, Kelsey H. Fisher-Wellman^{1,2,*}, and P. Darrell Neuffer^{1,2,3,*} 

From the ¹East Carolina Diabetes and Obesity Institute, ²Department of Physiology, ³Department of Biochemistry and Molecular Biology, Brody School of Medicine, East Carolina University, Greenville, North Carolina, USA

Edited by Qi-Qun Tang

Biological energy transduction underlies all physiological phenomena in cells. The metabolic systems that support energy transduction have been of great interest due to their association with numerous pathologies including diabetes, cancer, rare genetic diseases, and aberrant cell death. Commercially available bioenergetics technologies (e.g., extracellular flux analysis, high-resolution respirometry, fluorescent dye kits, etc.) have made practical assessment of metabolic parameters widely accessible. This has facilitated an explosion in the number of studies exploring, in particular, the biological implications of oxygen consumption rate (OCR) and substrate level phosphorylation *via* glycolysis (i.e., *via* extracellular acidification rate (ECAR)). Though these technologies have demonstrated substantial utility and broad applicability to cell biology research, they are also susceptible to historical assumptions, experimental limitations, and other caveats that have led to premature and/or erroneous interpretations. This review enumerates various important considerations for designing and interpreting cellular and mitochondrial bioenergetics experiments, some common challenges and pitfalls in data interpretation, and some potential “next steps” to be taken that can address these highlighted challenges.

In recent decades, a multitude of genetically modified cells and organisms have been developed with the aim of elucidating etiological and/or pathophysiological mechanisms of disease (1–3). These model systems often demonstrate features of modified or compromised energy metabolism (4–6). Recent technological advances and widespread commercial availability of instrumentation and reagents have facilitated an explosion of investigations into the consequences of gene variance in metabolic systems, with emphasis placed on processes related to cellular energy transduction through mitochondrial oxidative phosphorylation (OxPhos) and substrate-level phosphorylation in glycolysis (7–10). These bioenergetics assays, exemplified by the widely popular phosphorescent probe-based extracellular flux analysis (EFA) (8, 9), have also found broad use in other areas of biomedical research. For example, EFA studies have contributed to significant advances in

identification of novel metabolic liabilities of common drugs (11, 12), high-throughput comparison of metabolic features of cancer-derived cell lines (13–15), and elucidation of the links between cell energy transduction and programmed death (16).

Though there has been great utility in the widespread application of bioenergetics assays to biomedical science, some assumptions regarding cellular metabolic organization persist that may ultimately impede scientific progress. These assumptions can be nuanced and likely persist because they can be made to be observable by experimental conditions. As examples, the “Warburg effect” in cancerous and noncancerous cells and mitochondrial “dysfunction” in metabolic diseases (e.g., type II diabetes mellitus) can both be detected depending on conditions, but both have physiological implications that remain disputed (17, 18). Additionally, common bioenergetics measurements have significant caveats that can dramatically impact the quality of their interpretations. For example, the ECAR to OCR ratios that are often used to “diagnose” the Warburg effect are subject to several modifiers that can impact their proportionality to the metabolic processes they are meant to represent (9, 10).

The purpose of this article is to provide an overview of cellular bioenergetics assay design, emphasizing key conceptual and practical considerations, as well as perspectives on some common pitfalls in data interpretation. Some key considerations in flexible bioenergetics assay design are covered in the first section, followed by additional discussion of three topic areas of general importance: 1) cellular energy and ATP, 2) glycolysis, ECAR, and energy partitioning, and 3) mitochondrial dysfunction.

Designing bioenergetics experiments

Experimental platforms

Nearly all bioenergetics studies take advantage of the principle of steady-state mass balance to determine metabolic fluxes. In this scheme, external and/or internal fluxes are measured, then the net flux is fit to a model of the metabolic system(s) under study, and the unknown fluxes are then estimated. The main discriminating factor among different approaches lies in the degree of molecular “resolution,” or the ability to distinguish accurately between pathways or individual reactions. The current experimental modality with the highest molecular resolution is metabolic flux analysis (MFA)

* For correspondence: P. Darrell Neuffer, neufferp@ecu.edu; Kelsey H. Fisher-Wellman, fisherwellmank17@ecu.edu.

(19). In this method, internal fluxes are measured by fitting isotopomer labeling patterns to a mass balance simulation of fluxes through a network model to interpolate individual reaction fluxes (20). Two alternative methods include respirometry and extracellular flux analysis, which involve time-resolved measurement of external fluxes only, paired with metabolic substrate and inhibitor protocols to reductively interpolate fluxes through specific reactions/pathways. These methods are low molecular resolution compared with MFA but are capable of measurements over short timescales, which is a limitation of MFA studies due to the typically long incubation times required to achieve an isotopic steady state (20). Because of technical challenges, MFA studies also tend to be performed by researchers with extensive experience in biochemistry/metabolism. Respirometry and extracellular flux analysis will be the continued focus of this review because of their broad use by researchers that do not necessarily specialize in bioenergetics research.

Measuring mitochondrial metabolic fluxes *via* oxygen consumption rate (*i.e.*, respirometry) has been used for decades and has been essential in the development of the modern understanding of mitochondrial physiology (21). In these experiments, cells/tissues/organelles in an enclosed chamber are exposed to defined conditions and oxygen tension in the media is measured over time. The structure and coupling stoichiometries of the electron transfer system (ETS) and energetically coupled transport processes are well characterized in a variety of cell types (22, 23). This allows the interpolation of metabolic flux through mitochondrial metabolic pathways (*e.g.*, OxPhos) from OCR data. There are two common methods currently employed to measure OCR: 1) a potentiometric method that uses a platinum hydrogen (Clark) electrode, and 2) quenching of the fluorescence lifetime of metalloporphyrin complexes (MPCs) by the presence of elemental oxygen (24, 25). Clark electrodes are widely used in commercial systems (*e.g.*, Oxygraph-2K; Oroboros) as well as in "homemade" apparatuses, and principles of their design and function are well described (26, 27). Solid-state MPCs are the most likely technology used in the extremely popular Seahorse Extracellular Flux Analyzer (Agilent technologies) (8), although that information has not been made explicitly available to the scientific community. MPCs can also be prepared/purchased in soluble form and their molecular design and function have been described (24, 25, 28, 29). ECAR is another external parameter that can be measured and interpolated to

metabolic flux. Like the methods employed in respirometry, this can be measured using fluorescence lifetime quenching of lanthanide-based small-molecule probes (30).

Several additional measurements are commonly used in conjunction with measured external fluxes. For example, measurement of the electrochemical potential across the inner mitochondrial membrane (IMM) is proportional to the energetic state of the ETS and can be measured potentiometrically or with fluorescent organic cations (*e.g.*, tetramethyl rhodamine methyl ester) (31, 32). The redox potential of the reduced pyridine nucleotide pool (NAD(P)H) within specific subcellular compartments can be proportional to the energetic state of specific pathways and can be monitored *via* autofluorescence (ideally fluorescence lifetime) (33, 34). Additionally, enzyme activity assays are cost-effective and relatively simple to perform and can be used in conjunction with other assays to provide information regarding specific reactions and/or to reveal allosteric interactions (34). Many other fluorometric probes are available for measuring pH and ion gradients in a variety of model systems (35, 36). There has also been significant advancement in design of genetically encoded probes that can report additional changes in internal conditions, for example, intracellular pH, GSH/GSSG ratio, NAD(P)H redox state, etc. (37–39). Finally, some platforms/instrumentation is best suited for specific types of preparations. Some of these considerations are highlighted in Table 1.

Buffer/media chemistry

A major consideration in the design of bioenergetics assays is the buffer (or media) chemistry. The media/buffer composition for intact cell *versus* permeabilized cells/isolated mitochondria is essentially opposite in ionic composition (*i.e.*, intact high sodium and calcium/low potassium; permeabilized-high potassium/low sodium and calcium). Intact cells placed in buffers designed for permeabilized cells/isolated mitochondria will likely be lysed due to the hypotonic nature of the buffer (and vice versa). Both ionic strength and osmolarity should be considered to avoid significant effects on the kinetics and energetics of metabolic pathways (40–42). Additionally, certain ions may modulate metabolic fluxes on their own, which could necessitate the use of salts with alternative (inert) ions. For example, sodium alters isolated mitochondrial respiration rates, which can be circumvented by using tris-based salts (34).

Table 1
Considerations for choosing instrumentation for extracellular flux analysis studies

Considerations	Potentiometric (electrode)	Solid-state phosphorescent probe	Soluble phosphorescent or fluorescent probe
Manufacturer	Oroboros O2K	Agilent Seahorse XF Flux Analyzer	Agilent Mito-Xpress and pH-Xtra
Format	Sealed Chamber(s)	Specialized Microplate	Standard (culture) microplate
Variables measured	OCR, Membrane Potential	OCR, ECAR	OCR, ECAR
Suitable for adherent cells?	No	Yes	Yes
Suitable for suspension cells/isolated mitochondria?	Yes	No	Yes
Suitable for permeabilized cells?	Yes	Yes	Yes
Measurement type	Kinetic	Kinetic (>4 Injections)	Serial

To further emphasize the impact of assay media conditions on tonicity and osmolarity, consider that many metabolic intermediates are multivalent ions, which contribute substantially to both parameters. For example, a 5 mmol/l addition of sodium citrate, imparts 20 mOsmol/l to the osmolarity and 30 mmol/l to the ionic strength of the buffer. Additionally, sodium citrate is a salt of a weak acid that may raise the pH and buffering capacity of the media, particularly in low or unbuffered media that is often used for ECAR measurements. To address this type of issue, reported buffer/assay media descriptions should include information regarding changes in these parameters over the course of the assay. Additionally, controls should be included to account for the relative contributions of these changes, for example: 1) metabolically inert sugar alcohols (*e.g.*, mannitol) to account for osmotic effects, 2) salts with alternative counterions in accordance with the type of preparation, or 3) inert weak acids with a pK_a similar to the metabolite under investigation to account for pH effects.

Substrate/inhibitor titration

Because respirometry and EFA are limited by low molecular resolution, experiments are typically designed to compensate by reductively separating out components of individual reactions or pathways and by measuring multiple related parameters to reduce ambiguity (34, 43, 44). The most common general strategy is known as substrate-inhibitor titration (SUIT). In this strategy, external flux is measured while "input" metabolite (substrate) for a given pathway is provided in increasing concentration until the saturating substrate concentration is reached. To obtain additional resolution, specific inhibitors of steps within the pathway are titrated to determine the degree of control exerted by those steps under that specific set of experimental conditions (45). This strategy is often necessarily implemented through multiple parallel experiments to obtain a more complete working picture of the metabolic system (34, 44, 46, 47).

Importantly, there is no single way to approach SUIT design, and flexible protocol design can be generalized to a few key steps: 1) define the pathway (metabolic network model), 2) identify experimentally measurable fluxes, 3) identify candidate substrate/inhibitor combinations to isolate flux through specific pathway components, and 4) determine the most appropriate statistical design for the specific comparisons of interest. Notably, each of these steps must be very carefully considered to avoid ambiguity in the resulting interpretations. Several articles and books have been published that serve as excellent starting points for SUIT design in isolated mitochondria, permeabilized cells/tissue, and intact cells (9, 10, 44, 46–50).

Energy substrate choice

Choice of substrates (*i.e.*, metabolic intermediates that support catabolic pathway flux) is significantly influenced by the model of the metabolic network under study. In permeabilized cells/isolated mitochondrial preparations, the metabolic systems are separated from their normal physiological context. This necessitates careful consideration of substrate choices because multiple

metabolites may need to be present to fully support the metabolic network or prevent feedback inhibition. As an example, fatty acid oxidation (FAO) in isolated skeletal muscle mitochondria cannot proceed in the absence of low (~ 0.1 mM) concentrations of malate, but can in liver mitochondrial preparations due to a different mechanism of relieving feedback inhibition by acetyl-CoA (44). Additionally, substrate transport may be influenced by several other factors including energy dependency of the transport process, substrate ionization state, substrate concentration, or cofactors required for symport/antiport mechanisms (51–54). For intact cells, transport of metabolites across the plasma membrane also adds an additional layer of complexity and some metabolites may require specific cofactors or growth factor stimulation for uptake (55). Ultimately the network model chosen by the experimenter must account for these factors, which will manifest differently depending on preparation type, as well as subculture conditions or cell type/tissue of origin.

Inhibitor choice

There are a large number of possible inhibitors that can be used to target specific reactions within metabolic pathways and reports/reviews that may aid in identifying appropriate compounds are readily available in the literature (56–58). There are a few considerations to keep in mind when choosing inhibitors for bioenergetics experiments: 1) not all inhibitors are permeable to all preparation types (*e.g.*, intact cells *versus* permeabilized cells/isolated mitochondria), 2) some inhibitors may be metabolized or transported out of cells, which can result in unstable kinetic effects, and 3) minimal effective inhibitor concentrations should be determined using titrations and curve fitting to determine the appropriate experimental concentration from the dose–response kinetics. Importantly, the details involved in choosing the inhibitor concentration should be reported when possible.

Normalization factor(s)

Another critical factor in the design of bioenergetics experiments is the choice of normalization factor(s). Metabolic flux through a given pathway will depend on the amount/activity of the enzymes and metabolic intermediates present in the sample, neither of which necessarily scales with other variables (*e.g.*, cell volume). Cell counts are sometimes used for normalization in intact cells. However, some experimental designs may require comparisons among cells that are physically different sizes and would thus have a different total cell mass for the same number of cells. A popular way to circumvent this challenge is to normalize flux data to protein concentration, which can be measured using a bicinchoninic acid assay (59). This strategy may present challenges in situations where enzymes participating in the metabolic pathway under study are outnumbered by other soluble proteins, which act as background noise in the assay. The same considerations apply to isolated mitochondria studies, with the additional challenge that cellular proteins may contaminate the mitochondrial preparation, which may skew normalization when comparing different tissue/cell types or conditions (60). Ultimately, there is no single optimal normalizing factor. Instead,

normalization must be carefully considered early in the experimental design and several options should be tested to determine the best approach.

Standardization and quality control

All bioenergetics experiments are subject to variability due to the mode of preparation. For intact cells, this may include growth conditions of the cells (*e.g.*, media formulation, incubation conditions), cell viability (especially in drug studies), and cell type/tissue of origin. For permeabilized cells and tissues, significant variability can be introduced by the permeabilization agent and procedure during tissue isolation/separation. Additionally, isolated mitochondria preparations are very sensitive to the isolation conditions, and obtaining undamaged mitochondria is not trivial. Finally, variation may be introduced due to drift in the instrumentation being used. To account for potential sources of variation, standardization practices should be incorporated into all bioenergetics designs (and reported when possible). The simplest way to standardize the effects of preparation on bioenergetics experiments is to develop abbreviated assay protocols that are not anticipated to vary so long as underlying conditions remain the same. Several previously described assay designs can be adapted for use as standard assays, including the popular "stress tests" often implemented in the xF analyzer platforms or the respiratory control ratios described for isolated mitochondria studies (9, 47). These can be performed repeatedly throughout the course of experiments to detect drift in preparation or instrumentation. To standardize drift in instrumentation, positive and negative control conditions can be created that test the dynamic ranges of the measurement. For example, glucose/glucose oxidase can be used to induce a high noncellular rate of oxygen consumption and cyanide can be used to completely inhibit most biological respiratory processes (29).

Additionally, due to the variability that preparation quality can introduce, it is important to include quality control assessments in assay design whenever possible. For example, damaged mitochondria may still respire, but at very low coupling efficiency with OxPhos, which can be assessed by using respiratory control ratios that determine the degree of kinetic control of OxPhos over total respiration (47). To account for mitochondrial damage, a cytochrome *c* titration is often performed to test the integrity of the outer mitochondrial membrane. Cytochrome *c* may also be limiting under certain assay conditions or physiological circumstances, necessitating its addition in the assay buffer (49). For intact cells, several cost-effective cell viability assay strategies are available and should be used in conjunction with qualitative morphological analysis to ensure that cells are healthy and viable. Note that some viability assays such as luciferase-based ATP assays or diaphorase activity-dependent assays (*e.g.*, resazurin or tetrazolium dyes) are sensitive to changes in cellular metabolism and should not be used as indicators of viability. Necrosis (permeability)-based assays such as ethidium homodimer-2 or propidium iodide are recommended.

Interpreting bioenergetics experiments

The preceding section highlighted key considerations regarding general design of bioenergetics studies. The following section addresses a few issues that commonly impact the interpretation of cellular bioenergetics studies. Experimental interpretations are not just sensitive to the caveats intrinsic to the measurements being made, but also to some of the assumptions that underlie the questions being asked. The following section will focus on four areas in which both issues have and continue to influence data interpretation: 1) cellular energy and the meaning of ATP measurements, 2) energy partitioning between glycolysis and OxPhos, 3) challenges underlying interpretation of ECAR measurements, and 3) whether differences in mitochondrial functional parameters are indicative of pathological "dysfunction," as well as strategies to discern when (or if) that is the case.

Cellular energy and ATP measurements

Though there are many energy transducing reactions within cells, adenosine triphosphate (ATP) is generally considered to be the premier energy intermediate (61). A very common strategy for approximating cellular energetic state is to associate a change in metabolic flux (*e.g.*, OCR and/or ECAR) with a reduction in total ATP concentration (often qualitatively denoted ATP "levels"), which is commonly measured using luciferase-based enzyme coupled reaction schemes. This association is often interpreted as a failure of metabolic flux to support a given physiological ATP concentration (62–64). However, there are several problems with this interpretation. First, ATP levels reflect the steady-state balance between the rates of ATP synthesis and ATP hydrolysis, and thus both must be considered. Second, there is a common misconception regarding how ATP acts as an energy intermediate in cells; specifically, that the energy "stored" by ATP is held within the gamma phosphate bond. The gamma phosphate bond is sometimes referred to as "high-energy," which is physically correct but colloquially misleading. The term "high-energy" refers to both charge repulsion and the fact that inorganic phosphate is resonance stabilized in aqueous solution (61). However, it is not the case that the bond itself "contains" energy, and it is certainly not the case that energy is released by breaking of the bond (a process that *requires* energy).

From a thermodynamic perspective, energy is transduced in proportion to the direction and extent of displacement of the ATP hydrolysis reaction rather than through the ATP molecule itself. Quantifying this relationship requires measuring concentrations of both the product (ATP) and reactants (ADP+P_i). The free energy of ATP hydrolysis can be expressed as a phosphate group transfer potential and quantitated by the Gibbs free energy of the hydrolysis reaction (ΔG_{ATP} , kJ/mol) (65, 66).

$$\Delta G_{ATP} = \Delta G^{\circ\prime}_{ATP} + RT \ln \Gamma = RT \ln \left(\frac{\Gamma}{K_{eq}} \right) \quad (1)$$

ΔG_{ATP} is empirically derived from the equilibrium (K_{eq}) and observed (Γ) mass action ratios of the reaction. $\Delta G_{\text{ATP}}^{\circ}$ is the Gibbs energy at physiological pH and temperature and R and T are the gas constant and absolute temperature, respectively. This equation demonstrates that the energy available from ATP hydrolysis is quantitated from its relative *displacement* from thermodynamic equilibrium, which in biological systems is held at a steady-state value dependent on the energetic and kinetic states of *both* catabolic (supply) and anabolic (demand) reactions (67–69).

In extreme situations, total ATP may be an indicator of cell health. In fact, the most popular luciferase-based assay, the cell-titer glo assay (Promega), is billed by the manufacturer as a viability assay, not as an energetic assay. A reduction in cellular ATP may indicate a reduction in the total adenylate pool due to purine degradation during energetic crisis or other physiologically relevant scenarios (70). However, if the energy status of the cell is what is being investigated, then a more comprehensive approach is required. The theoretical ATP hydrolysis mass action ratio is challenging to measure due to the many ionic forms of reactants and products involved in the gross reaction (69). However, in the early 1970s, Atkinson and Chapman proposed a practical "shorthand" mass action ratio involving free ATP, ATP + ADP, and total adenylates measured using enzyme coupled reactions (71, 72). This (rudimentary) approach offers an improvement over measuring ATP levels alone, as it leverages the same concept as commercial luciferase kits. It also accounts for the ATP hydrolysis mass action ratio and is not significantly more difficult to perform. Alternatively, the ATP hydrolysis mass action ratio can be determined using high (or ultra) performance liquid chromatography (73). Note that in this case, free ADP is difficult to measure because it is present in very low concentrations, and extraction methods often capture ADP that was not actually free within the cell, but rather, bound to cellular proteins. Approaches that leverage the known equilibrium constant of the creatine kinase reaction, along with HPLC measurement of other phosphagens, may be used to calculate free ADP concentrations in some tissues (73).

The rate of ATP turnover (J_{ATP}) is another representation of the cell's energetic phenotype that compliments static measurements of the ATP mass action ratio. It is directly proportional to the power transferred through the phosphate potential (Box 1), which if measured over the duration of a cellular process is proportional to the total work required by the process itself (74). Directly measuring J_{ATP} is complex and limited by technical challenges (75), but *estimating* J_{ATP} from EFA data is straightforward and has been recently described in detail (9, 10, 31). Importantly, there is a major caveat to this approach: *i.e.*, the quality of the estimation is only as good as the assumed reaction coupling stoichiometries for a given metabolic pathway, and the model of the pathway is ultimately up to the experimenter. It can be very difficult to determine the coupling stoichiometries explicitly in intact cells because it is not always possible to isolate specific substrate oxidation patterns. For example, a sample of intact cells may oxidize stored carbohydrates and fatty acids simultaneously,

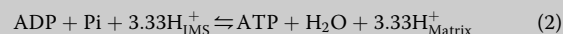
Box 1. Mitochondrial energy transduction and power output

In the standard model of mitochondrial energy transduction (43, 210, 211): 1) organic molecules (*i.e.*, fuels) transfer electrons through a series of coupled redox reactions that terminate on the reduction of O_2 to H_2O ; 2) this series of redox reactions is coupled with proton translocation to the intermembrane space, resulting in a rapid equilibration of other permeant ions and counter ions that constitutes an electrochemical potential; 3) the electrochemical potential (or proton motive force, pmf) is dissipated through membrane-bound enzyme complexes (*e.g.*, ATP synthase) in order to perform useful work. For additional visualization, this concept has also been described through several didactic analog models (47, 212–214).

The potential energy of each step is constrained by the maximum transfer potential of the previous step, which depends on both the magnitude of the "driving" force as well as the stoichiometry of the process (212).

$$\Delta G_{\text{Redox} \rightarrow \text{pmf}} = \Delta G_{\text{Driving}} + \Delta G_{\text{Driven}} = -2F(E_{\text{h}}^{\text{O}} - E_{\text{h}}^{\text{NADH}}) + 10\Delta G_{\text{pmf}} \quad (1)$$

This equation demonstrates the maximal work transfer from the combined redox reactions of the ETS to the proton motive force (pmf) for a two-electron transfer from NADH to oxygen. O indicates $\frac{1}{2}$ mole O_2 , F is Faraday's constant (converts from Volts to J/mol). The stoichiometric coefficient 10 comes from assuming a proton pumping stoichiometry of 4, 4, and 2 for respiratory complexes I, III, and IV, respectively (27, 215–217). The pmf derived from the entire redox span ($\text{NADH}:\text{O}_2$) is approximately -185 mV or 17.8 kJ mol^{-1} , assuming that the steady-state redox potential of the ETS is -925 mV (43, 168). ADP phosphorylation by the mammalian F_0F_1 ATP synthase enzyme complex is thought to phosphorylate ~ 3 ADP from ~ 10 protons transferred from the intermembrane space (IMS) toward the matrix, resulting in a final stoichiometry of ~ 3.33 mol $\text{H}^+ \cdot \text{mol}^{-1}$ ATP (22, 218):



The Gibbs energy differential from pmf to ADP phosphorylation can be determined by:

$$\Delta G_{\text{pmf} \rightarrow \text{ATP}} = 3.33\Delta G_{\text{pmf}} + \Delta G_{\text{ATP}} \quad (3)$$

Thus, the estimated *maximum* work that the full redox span from NADH/NAD^+ to $\text{O}_2/\text{H}_2\text{O}$ can transfer to the ATP phosphate group transfer potential (for this specific value of ΔG_{redox}) has a magnitude of $3.33 \cdot 17.8$ kJ $\text{mol}^{-1} = 59.2$ kJ mol^{-1} . If the magnitude of driven force drops due to net ATP hydrolysis (demand), the driving force will tend toward this value, so long as the ETS redox potential (supply) remains unchanged.

Thermodynamics describe the direction and extent of biochemical reactions, but these expressions do not contain any kinetic information. Steady-state kinetics of mitochondrial energy transduction are similarly constrained by flux through preceding and succeeding steps as well as the coupling stoichiometries of the individual reactions that comprise the system (34). Work (or energy) transferred per unit time is denoted as power and has SI units of Watts ($\text{J} \cdot \text{s}^{-1}$). Power is an extremely useful parameter because it encompasses both kinetic and energetic information and is capable of supplying information regarding the actual quantities of work required to perform cellular processes (*i.e.*, by integrating the power over the time course of the process) (74). If a sample of a known quantity of isolated mitochondria or permeabilized cells respire on pyruvate/malate, then electron transfer to the CoQ/CoQH_2 redox couple can be attributed to only NADH linked redox transfer through respiratory complex I (34). The ATP/O stoichiometry is approximately:

$$\frac{10 \left(\frac{\text{H}^+}{\text{O}} \right)}{3.33 \left(\frac{\text{H}^+}{\text{ATP}} \right)} = 3.0 \left(\frac{\text{ATP}}{\text{O}} \right) \text{ or } 6.0 \left(\frac{\text{ATP}}{\text{O}_2} \right) \quad (4)$$

If ΔG_{ATP} is -59.2 kJ mol^{-1} , which represents a moderate to high cellular energetic demand state (34), then an equivalent $+59.2$ kJ mol^{-1} work transfer is required to maintain it. If mitochondria respiring against a $\Delta G_{\text{ATP}} = -59.2$ kJ $\cdot \text{mol}^{-1}$ have a measured steady-state respiration rate of $J_{\text{O}_2} = 4.5$ nmol $\text{O}_2 \cdot \text{s}^{-1} \text{mg}^{-1}$ mitochondrial protein (34), the ATP phosphorylation rate can be calculated:

$$6.0 \left(\frac{ATP}{O_2} \right) * 4.5 \text{ nmol } O_2 \cdot s^{-1} \cdot \text{mg}^{-1} = 27.0 \text{ nmol } ATP \cdot s^{-1} \cdot \text{mg}^{-1} \quad (5)$$

The steady-state work transfer rate to the phosphate potential is:

$$27.0 \text{ nmol } ATP \cdot s^{-1} \cdot \text{mg}^{-1} * 5.92 * 10^{-5} \text{ J} \cdot \text{nmol } ATP^{-1} \\ = 1.6 * 10^{-3} \text{ J} \cdot s^{-1} \cdot \text{mg}^{-1} = 1.6 \text{ mWatts} \cdot \text{mg}^{-1} \quad (6)$$

In the case of an alternative fuel source with a different ATP/O ratio, such as isolated mitochondria respiring in the presence of succinate/rotenone (34), the electron transfer to the CoQ/CoQH₂ redox couple can be attributed to only FADH₂ linked redox transfer through respiratory complex II (34). This results in only 6 H⁺/O for the entire redox span, and the ATP/O₂ ratio changes to:

$$\frac{6 \left(\frac{H^+}{O} \right)}{3.33 \left(\frac{H^+}{ATP} \right)} = 1.8 \left(\frac{ATP}{O} \right) \text{ or } 3.6 \left(\frac{ATP}{O_2} \right) \quad (7)$$

To maintain the same rate of ATP phosphorylation (*i.e.*, the same power output), the estimated respiration rate would need to be approximately 7.5 nmol O₂ · s⁻¹ · mg⁻¹. This is congruent with experimentally determined values using isolated mitochondria from mouse hearts (Fig. 7) (34). Together these examples illustrate a critical bioenergetic concept: two different catabolic substrates exhibit different rates of respiration but support the same power output. Even though it may be tempting to assign "dysfunction" to any condition that results in slower respiration rates, these observations may simply represent a common metabolic strategy that ensures consistent power output (108).

which are predicted to have different ATP/O stoichiometries in OxPhos (10). In this case, SUITs could be designed to isolate oxidation patterns of specific substrates with known stoichiometries in mitochondria isolated from the intact cells, and the ATP/O stoichiometry could be measured directly under the same substrate conditions (34, 41, 76, 77). Parallel experiments could then be performed to measure oxidation patterns in the intact cells using nutrient-restricted media or inhibitors designed to reduce ambiguity in the substrates being oxidized (31).

To the best of our knowledge, no similar approach is available for isolating substrate level phosphorylation stoichiometries in glycolysis, which would likely necessitate the use of isotopomer-based metabolic flux analysis (78, 79). This is important because: 1) not all hexose equivalents will enter the ADP phosphorylating steps of lower glycolysis in intact cells (80, 81), and 2) lactate is likely oxidized in the mitochondria of many cell/tissues, which means that the ECAR may not be directly proportional to substrate level phosphorylation of ADP (82). For these reasons, ECAR measurements must be very carefully interpreted, which is discussed in greater detail in the next section.

Cellular energy partitioning between glycolysis and OxPhos

Despite the importance of the ATP hydrolysis reaction in the function of many cells, the number of biochemical pathways that result in net phosphorylation of ADP are surprisingly sparse. The two most well-understood energy transducing reaction schemes are OxPhos and substrate level phosphorylation in glycolysis. There is a well-known difference in molar efficiency between OxPhos and substrate-level

phosphorylation (*i.e.*, ~38 mol of ATP/mol glucose *via* OxPhos, 2 mol ATP/mol glucose in substrate level phosphorylation in glycolysis), which is often used as a basis for classifying the energetic economy of cells. EFA technologies have facilitated an explosion in studies that compare the relative contributions of these two pathways to cellular energetic states. The comparisons made often include multi-parametric "stress" tests that use SUITs to assess several flux parameters (64, 83, 84). Additionally, the ratio of OCR/ECAR is popularly used as an index of cellular bioenergetic function (85, 86). However, the interpretation of some of these parameters, particularly OCR/ECAR, can be quite problematic. The problems arise from two important issues: 1) OCR/ECAR is not quantitatively related to any metabolic fluxes, and 2) the physiological meaning of a shift in flux between these two pathways is complicated and can be artifactually created by the assay conditions.

Challenges underlying interpretation of ECAR measurements

Assumptions about the meaning of OCR/ECAR stem from the so-called "Warburg Effect" but may not be meaningful

In the 1920s, Otto Warburg famously observed that Ehrlich ascites tumors produced venous blood lactate under normoxic conditions (87). He later hypothesized that this observation could be caused by intrinsic damage to cellular respiration, citing the observation that other common causes of respiratory damage result in a similar metabolic phenotype (*i.e.*, ischemia/reperfusion and exposure to respiratory poisons) (88). At the time, it was a very reasonable hypothesis, because fermentation was being heavily studied in yeast and skeletal muscle, neither of which performs extensive fermentation under aerobic conditions. Warburg's hypothesis has persisted (inconclusively) for nearly 70 years and has continued to be broadly associated with cancer despite the lack of consensus model, mechanism, or consistent evidence of therapeutic potential (17, 80, 89–91). The acceptance of the Warburg hypothesis as an "effect," seems to have also inadvertently led to persistent generalizations regarding the relationship between central carbon metabolism and cellular energy partitioning even in noncancerous cells (17). More specifically, it has reinforced the notion that some cells may "prefer" either aerobic or anaerobic glycolysis in support of their energy metabolism, and that this "preference" indicates metabolic inefficiency if the "anaerobic" pathway prevails under normoxic conditions (13).

The biochemical "logic" underlying glycolytic energy transduction has been very nicely reviewed by Bar-Even *et al.* (92). In summary, a hexose (typically glucose) is phosphorylated, isomerized, and enzymatically cleaved, ultimately resulting in 2 M equivalents of triose phosphate. In "lower" glycolysis, these triose phosphate equivalents undergo two major electron rearrangements, which provide the net driving force for substrate-level phosphorylation of ADP. Mass action ratios of glycolytic intermediates and calculations of pathway energetics have been assessed under resting conditions in erythrocytes (which notably lack mitochondria) and other subcultured cell lines (79, 93, 94). In those studies, substrate-

level phosphorylation supported a steady-state ΔG_{ATP} between approximately $-50 \text{ kJ} \cdot \text{mol}^{-1}$ and $-59 \text{ kJ} \cdot \text{mol}^{-1}$, which are similar (albeit lower on average) compared with ΔG_{ATP} supported by OxPhos (34, 41, 66, 77). This supports the notion that, under certain conditions (e.g., hypoxia or ETS inhibition), homolactic fermentation may support the energy metabolism of some cell types. For example, this phenomenon has been well described in ρ^0 cells that have been depleted of mitochondria *via* chronic inhibition of mtDNA replication (95).

Sole reliance on fermentative energy metabolism would certainly impose significant kinetic constraints on the required flux through carbohydrate metabolism, but such an effect may only be meaningful when high-power output is required over sustained periods of time. Indeed, this likely explains why genetic diseases that affect mitochondria disproportionately impact tissue types that undergo sustained increases in power output as part of their physiological function (e.g., striated muscle and neurons) (96). Thus, the limitations on cellular function imposed by energy homeostasis depend in large part on the physiological activities of the cell type, as well as the specific metabolic constraints determined by the cell's microenvironment (e.g., nutrient availability and/or regulation of nutrient uptake) (60, 97–99). The extent to which this limitation applies to cell/tissue types that do not depend on high-power output is less understood. Unfortunately, it is not uncommon for assumptions about the energetic requirements of cellular processes to be implied with very little (if any) supporting evidence. The energetic requirement of cell proliferation in cancer is one prominent example and is often assumed to be highly dependent on ATP demand (84, 100, 101). However, findings from several recent investigations indicate that cancer energetics are much more nuanced, and that other energy intermediates such as reduced pyridine nucleotides may be more limiting than ATP in essential macromolecular synthesis reactions that limit proliferation rate (102–104).

A more modern view of the balance in energy partitioning between OxPhos and substrate-level phosphorylation hinges on several important observations. First, both OxPhos and glycolysis transduce chemical energy while simultaneously providing molecular "backbones" and reducing equivalents for anabolic reactions (termed amphibolism) (103–107). This is important because either of these requirements may constrain flux depending on the context/conditions. For example, the "warburg effect" in cancer has been proposed to be a by-product of maintaining high flux through the pentose phosphate and 1-carbon metabolism pathways, which may be more important for mitosis than supporting a high rate of ATP turnover (80, 102). Second, cells likely balance the energetic and kinetic trade-offs between the two pathways to ensure consistent power output and may use subcellular localization of mitochondria or glycolytic "metabolons" to support specific processes such as maintenance of transmembrane ion gradients (108, 109). Finally, flux through glycolysis and OxPhos are integrated through electron "shuttling" pathways such as the malate-aspartate shuttle (MAS). Though the MAS is often depicted as a way to deliver "excess" electron equivalents to the ETS, this process is actually *energy-dependent* due to

electrogenic transport of neutral glutamic acid for anionic aspartate (54, 110, 111). Manipulating MAS has been shown to induce complex effects in both OxPhos and glycolysis in several cell types, further highlighting that electron shuttling reaction schemes serve as points of integration between the two pathways (112, 113).

Challenges of interpreting ECAR and ECAR/OCR ratio data and some suggested strategies for overcoming these limitations

Homolactic fermentation produces two net lactate anion equivalents from a hexose equivalent. Monocarboxylate transporters on the plasma membrane may then transport lactate out of the cell *via* an electroneutral lactate/ H^+ symport mechanism, which results in net acidification of the external microenvironment (51). Thus, in minimally buffered media, ECAR is *proportional* to the rate of lactate efflux resulting from homolactic fermentation (Fig. 1A). This measurement is typically included in EFA studies, but is very often misinterpreted as being a direct measure of "glycolytic flux" (85, 86). Importantly, the proportionality of ECAR with glycolytic flux can be confounded by other sources of extracellular acidification. Additionally, typical ECAR units (mpH/min) are not stoichiometrically related to any metabolic fluxes (*i.e.*, how many ATP/mpH/min are expected to result from glycolysis?) (114).

It is generally assumed that all lactate produced in glycolysis will be effluxed (Fig. 1B). However, a recent radioisotope labeling study in mice determined that circulating lactate turnover was the highest of all blood metabolites, resulting in labeling of a variety of TCA cycle intermediates in all tissues tested (82, 115). Additionally, mitochondria isolated from many cells and tissues have been shown to oxidize lactate at rates that are similar to (or greater than) pyruvate (111, 116–118). Lactate dehydrogenase reactions tend to favor lactate

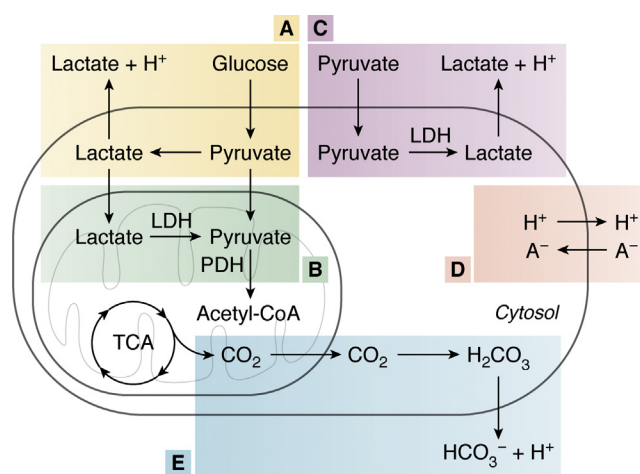


Figure 1. Potential sources of error in ECAR measurements. A, homolactic fermentation may result in symport of lactate/ H^+ , making ECAR proportional to substrate-level phosphorylation in glycolysis. B, oxidation of lactate in mitochondria may result in glycolytic flux that is not detectable through ECAR. C, exogenous pyruvate may be reduced to lactate without being directly coupled to glycolytic flux. D, ECAR may be unrelated to lactate/ H^+ symport (e.g., alternative anion/ H^+ exchange mechanisms). E, CO_2 derived from respiration may induce acidification due to accumulation through bicarbonate and carbonic acid equilibrium.

formation from pyruvate at equilibrium under physiological conditions ($\Delta G^{\circ}_{LDH} = -23.4 \text{ kJ mol}^{-1}$) and LDH isoforms generally exhibit high activity (111). At relevant concentrations of reaction intermediates *in vivo*, the LDH reaction operates close to thermodynamic equilibrium, implying that the direction and extent of the reaction are sensitive to modulation by changing lactate, pyruvate, or NADH/NAD⁺ concentrations. This is particularly important for studies involving subcultured cells because it suggests that substrate conditions will likely affect the oxidation rate of lactate and thus skew the interpretation of EFA studies.

ECAR units can be made to be more stoichiometrically useful by conversion to a proton efflux rate (JH^+ ; a.k.a proton production rate- PPR) by empirically determining the buffer capacity of the media *via* titration of known amounts of strong acid (31, 114). This conversion is useful because JH^+ can be linked to the substrate-level ATP phosphorylation rate (APR_{Glyc}) *via* the following expression (10).

$$APR_{Glyc} = JH^+ \cdot \left(\frac{ATP}{H^+} \right) \cdot Q \quad (2)$$

where $\left(\frac{ATP}{H^+} \right)$ is generally considered to equal 1, and Q is a unitless proportionality constant that must account for the apparent coupling efficiency of JH^+ with substrate-level phosphorylation (9). In other words, Q represents the percentage of JH^+ that is linked to substrate level phosphorylation. This can be difficult to determine because it can be influenced by several factors (discussed above). However, a good place to start would be to begin the assay in the absence of exogenous lactate and measure the effluxed lactate at the end of the assay using an enzyme coupled reaction (*e.g.*, the hydrazine sink method) (119). Assuming that lactate is effluxed at a constant rate, the correction factor can be applied to JH^+ (9). This does, however, leave two remaining sources of error. First, in some cell types (*e.g.*, mammalian spermatozoa), the LDH reaction produces lactate from exogenous pyruvate independent of flux through lower glycolysis (Fig. 1C) (120). The extent to which this occurs in other cell types is not known. Thus, control experiments may need to be performed in the presence of an inhibitor that targets reactions of glycolysis (*e.g.*, α -chlorohydrin or 3-bromopyruvic acid; 2-deoxyglucose is not recommended due to confounding osmotic stress) or in the absence of exogenous pyruvate. Second, as mentioned above, lactate produced from homolactic fermentation may be oxidized in mitochondria, which would have the effect of "uncoupling" JH^+ from glycolytic flux. Whether or not a given cell type retains the ability to oxidize lactate in support of cellular respiration is testable using isolated mitochondria or permeabilized cell preparations (111, 116). Unfortunately, controlling for the magnitude of this effect in the intact cell to correct the ECAR measurement does not appear to be possible without altering the integration of OxPhos and glycolysis, because inhibiting lactate oxidation would likely alter glycolytic flux. Thus, further study would be helpful in this area.

Another caveat to ECAR measurements is that Lactate/H⁺ symport may not be the only source of H⁺ exchange (Fig. 1D). In a closed system near physiological pH, 1 mol of glucose will produce 6 mol of CO₂ if completely oxidized. Each mole of CO₂ generated will produce a molar equivalent of H⁺, therefore the CO₂ produced by oxidation of substrates in the TCA cycle can contribute substantially to ECAR through reaction equilibrium with bicarbonate and carbonic acid (Fig. 1E) (9, 114). The CO₂ contribution to ECAR is far from trivial and reported increases in ECAR are very often accompanied by increases in OCR that may confound the ECAR interpretation. This effect may be accounted for by leveraging a mathematical correction factor, described by Mookerjee *et al.* (9), which estimates CO₂ contribution to ECAR. Assays can also be performed in the presence/absence of purified carbonic anhydrase, which speeds the rate of CO₂ to carbonic acid equilibration (121). This will ensure that the rate of CO₂ hydration is not limiting, which could result in overestimation of the CO₂ contribution to the acidification rate (9). In a final word of caution, some cell types (*e.g.*, adipocytes, polarized-epithelial cells, osteoclasts, etc) acidify their environments as part of their normal physiological function, and many cells exchange free acid for cations (*e.g.*, Na⁺/H⁺ antiport), which may necessitate the use of additional controls (121).

Nonphysiological assay conditions may create artifactual glycolytic flux states

A major challenge in bioenergetics studies is that assay conditions themselves often create artifactual conditions that demonstrate questionable physiological relevance. Glycolysis has been extensively studied in a variety of cells and tissues, and nearly every enzyme in the pathway has been identified in one study or another as either energetically or kinetically limiting to overall pathway flux (122). Importantly, under normal physiological conditions, glycolysis does not appear to be regulated by cellular energetic demand. A recent study by Tanner *et al.* systematically overexpressed each catalyzing step in the glycolytic pathway and combined metabolic flux analysis with metabolic control analysis in two mouse cell lines (45, 78). It was determined that glycolytic flux control under basal conditions was exerted at only four reactions: glucose transport, the hexokinase reaction, the phosphofructokinase reaction, and lactate transport (*i.e.*, *via* the monocarboxylate transporter). Interestingly the ADP phosphorylating reactions of "lower" glycolysis did not exert control under resting cellular conditions. This is similar to another metabolic control study performed in primary rat hepatocytes that determined the majority of glycolytic flux control was exerted by glycolytic enzymes (*i.e.*, ~66% by enzymes, ~47% by ATP hydrolysis rate) (123).

However, control of flux in energy transducing systems is highly sensitive to conditions, and inhibition of a step within a given pathway can result in redistribution of control to the inhibited step (45). Under extreme conditions, such as exposure to the F-Type ATP synthase inhibitor Oligomycin A,

glycolytic flux exhibits an increase in net driving force as well as flux through the pathway, indicating sensitivity to increased energetic demand similar to kinetic regulation by adenylates observed in the OxPhos system (79, 124). Increased ECAR is commonly observed response to OxPhos inhibitors (e.g., oligomycin, antimycin A, Rotenone, etc.), which is interpreted to represent compensatory flux through aerobic fermentation in support of the phosphate potential. However, this condition does not strictly represent any physiologically meaningful steady state and instead creates artifactual changes in flux that do not necessarily provide information about physiological energy partitioning. Additionally, in cells with active electron-shuttling systems (e.g., malate aspartate shuttle), inhibiting the ETS may affect glycolytic flux through the cytosolic NAD⁺/NADH redox potential, which may change glycolytic flux kinetics independent of energetic demand (110, 112, 125).

With these considerations in mind, how can assumptions about energy partitioning among OxPhos and glycolytic substrate-level phosphorylation be addressed moving forward? Abandoning the simplified view that cellular energy transducing pathways are independent is a recommended start. Instead, research should focus on metabolic system integration and adaptation under experimental conditions conducted in the most physiologically relevant micronutrient environment that can be reasonably achieved (10, 31, 126). Non-physiological metabolic states may inform the limitations of the assay, aid in standardizing among replicates, or aid in interpolating a model of rate limiting steps in the pathway (45). However, buzzwords such as "max glycolytic capacity" and OCR/ECAR index simply are not meaningful and should not be used to compare experimental treatments or group effects unless this practice can be clearly justified under the circumstances.

Mitochondrial function and "dysfunction"

The details regarding the measurement of specific parameters related to mitochondrial function and OxPhos are quite numerous/complex and have been the subject of several books and reviews (21, 43, 44, 46, 47, 127, 128). Typical assays for assessing OxPhos in isolated mitochondria were developed in the 1950s and have remained surprisingly similar to the manner in which they were first described (21, 23). Standardized respiratory states are commonly achieved *via* saturating substrate conditions in the absence of ADP (State 4; Low respiration rate- JO_2), in the presence of ADP (State 3; High JO_2), or *via* addition of ATP synthase inhibitors and protonophore uncouplers such as Oligomycin and Carbonyl cyanide-p-trifluoromethoxyphenylhydrazone (FCCP; state u; High JO_2). Additional resolution is often achieved by using combinations of substrates and inhibitors to isolate activities of specific ETS complexes (44).

Intact cell measurements became fairly standardized with the advent of EFA and typically involve basal respiration as well as "max" or "uncoupled" respiration induced by a cell permeable protonophore (e.g., FCCP), which are often reported with calculated "ATP-linked" respiration (*i.e.*, basal –

oligomycin) and "respiratory reserve capacity" (*i.e.*, "max" – basal) (129, 130). Mitochondrial membrane potential measurements are also often included with both experimental preparation types (130). Methods typically involve use of a cationic indicator molecule that equilibrates with the steady-state voltage potential across the IMM (131–135). As was the case for OCR/ECAR, interpretation of mitochondrial functional parameters hinges on several important assumptions about the organization of the system as well experimental caveats that should be carefully considered. This is perhaps most relevant when attributing physiological effects to mitochondrial pathology or the more nebulous (and arguably less useful) term "dysfunction."

Assumptions about mitochondrial dysfunction stem from observed changes/differences in functional parameters that may not be meaningful

Bioenergetics studies often identify functional changes in mitochondrial metabolism (e.g., reduced respiration, membrane potential, etc) and then interpret these changes through a lens of mitochondrial pathology, leading to the conclusion that many diseases are mediated by some degree of mitochondrial dysfunction (96, 136–138). However, there are a few problems with this practice. First, mitochondrial dysfunction is not really a testable condition because it lacks a consensus definition. Second, and perhaps more importantly, changes in mitochondrial functional parameters often simply reflect the underlying energetic and kinetic flexibility of the system rather than a *bona fide* mitochondrial pathology (43).

A good way to illustrate this point is through brief discussion of the debate regarding the role of mitochondrial dysfunction in the etiology of skeletal muscle insulin resistance (IR) and glucose intolerance that arise as a consequence of obesity and type II diabetes mellitus (18). A popular hypothesis regarding the etiology of IR in skeletal muscle emerged in the early 2000s stemming from the work of Shulman and others (139). This hypothesis stipulated that ectopic accumulation of proinflammatory lipids (e.g., acyl-CoAs, diacylglycerol, and ceramides) occurs because of dysfunctional mitochondrial β -oxidation, which ultimately results in stress-dependent serine kinase activity that antagonizes insulin signaling (140). The proposed mitochondrial dysfunction was suggested to be the result of age- or environment-related decline based on observations of reduced rates of TCA cycle flux and ADP phosphorylation at rest in elderly IR patients *versus* young weight-matched controls (141). However, from simple bioenergetic principles, a decrease in mitochondrial function at rest should have minimal impact on the ability to oxidize fatty acids because the capacity of mitochondria to oxidize substrates is far in excess of what is needed at rest. Experimentally, several transgenic models in rodents have recapitulated loss-of-function in muscle mitochondrial β -oxidation, which results in ectopic lipid accumulation but not IR (142, 143). Additionally, reductions in state 3/state u respiration were not detected at the onset of IR in humans, and observations in rodent models have demonstrated that *in vitro* reductions in

respiratory kinetics and changes in mitochondrial ultrastructure/content follow (rather than precede) development of IR, indicating that these changes are simply adaptive in nature (144–146).

The connection between overnutrition and the development of IR is more likely mediated by substrate competition among fatty acid and glucose oxidation pathways, which is a manifestation of straightforward metabolic flux balance and allosteric feedback regulation of reaction kinetics by metabolic intermediates (147–150). In other words, these effects can be reasonably explained by the core principles of bioenergetics, rather than the presence of underlying mitochondrial pathology. More specifically, overnutrition results in an "oversupply" of catabolites, and mitochondrial energy transduction systems are energetically and kinetically limited by demand when supply is not limiting (18, 43, 151). Reduced rates of respiration can be normal (or even beneficial), rather than pathological, but to appreciate why requires an understanding of a few fundamental bioenergetics concepts (Box 1).

Overnutrition stimulus has been shown to be followed by adaptive reorganization of mitochondrial enzyme activity and/or content that manifests as a reduction in intrinsic mitochondrial functional parameters (*i.e.*, in isolated mitochondria that are removed from nutritional conditions of the cell) (152, 153). This effect has even been shown to occur in well-trained noninsulin-resistant individuals placed on a high-fat diet for just 5 days (154). But why would an *in vivo* shift in substrate oxidation patterns cause this effect? Though the ATP/O ratios for carbohydrate oxidation and β -oxidation are similar (~ 2.78 versus ~ 2.45 respectively), the molar ATP equivalents produced from complete β -oxidation are nearly fourfold higher (10). This also means that the number of electrons donated to the ETS per mole of substrate is also about fourfold higher. Additionally, β -oxidation donates ~ 2.4 times more electron equivalents to the CoQ/CoQH₂ redox couple, which is not directly linked to the thermodynamic "backpressure" of proton pumping through complex I. These consequences of metabolic organization result in the production of superoxide because the demand remains unchanged, but the input "pressure" from supply is increased (34, 155). Mitochondrial H₂O₂ production/emission (derived from superoxide) in turn is directly linked to the development of insulin resistance (156–159). Reactive oxygen species (ROS) have been demonstrated to induce rapid changes in various ETS enzyme activities through post-translation modifications, and Guaras *et al.* showed that complex I is degraded under conditions that result in a hyperreduced CoQ/CoQH₂ redox couple (160, 161). Both effects would be expected to manifest in conditional reductions in respiratory kinetics in isolated mitochondria or intact cell preparations, but these changes should be considered homeostatic rather than pathological.

There is no doubt that mitochondria play a critical role in the physiology of many cell types. Mitochondria-derived pathologies have been experimentally induced by genetic disruption of mitochondrial ultrastructure (162, 163) or toxic effects of small molecules on mitochondrial metabolism (164, 165). Though similar associations have been inserted into the etiology of

several diseases (*e.g.*, cardiovascular disease, neurodegeneration, and cancer), the interpretation of those data generally suffer from the same ill-defined causality as that promoted for the association of mitochondrial dysfunction with insulin resistance (136, 166, 167). To confidently conclude pathology, experiments must be designed to test the hypothesis that changes in mitochondrial functional parameters or cellular energy status precede the development of the disease phenotype.

Challenges involved with interpreting mitochondrial functional parameters and some suggested strategies for overcoming these limitations

Different types of preparations (*i.e.*, isolated mitochondria/permeabilized cells (IM/PCs) versus intact cells) have major differences in both experimental design and interpretation. IM/PCs offer more control over the specific biochemical conditions that regulate mitochondrial metabolism, but lack physiological context (47). IM/PC assay conditions are typically designed to saturate OxPhos kinetics (48), which can be useful for determining rate limiting steps when combined with inhibitor titrations but may also be susceptible to misinterpretations because the conditions are not reasonably recapitulated in live cells. Intact cell conditions are more physiologically relevant but limit unambiguous interpretation due to the complex and integrated nature of whole cell metabolic systems. Thus, interpreting data from either preparation type alone involves trade-offs between physiological relevance and experimental tractability (Fig. 2).

Nonphysiological metabolic states and artifacts

As mentioned earlier (Box 1), mitochondrial energy transduction can be modeled as an energetic and kinetic balance among four network control nodes (or modules) (34, 47). These include: 1) substrate oxidation by matrix dehydrogenases (energy supply), 2) coupling of the ETS redox reactions ETS with proton "pumping," 3) the electrochemical potential ($\Delta\Psi_m$; energy intermediate), and 4) $\Delta\Psi_m$ dissipating processes (energy demand). Importantly, these nodes are kinetically and energetically linked, and a change in a parameter that reports on only one node cannot be interpreted unambiguously without having additional information about

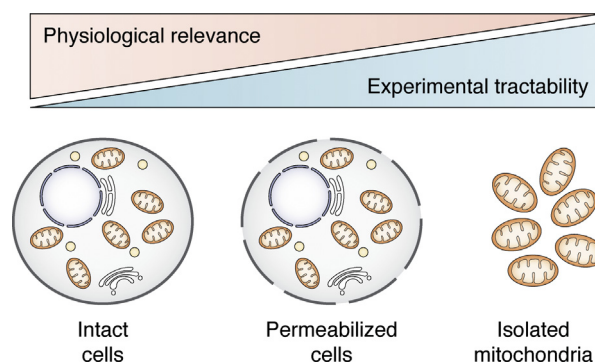


Figure 2. Experimental versus physiological tradeoffs made when using intact cell, permeabilized cell, or isolated mitochondria preparations to study bioenergetics.

the other nodes. Thus, the ideal approach to defining mitochondrial function under a given set of conditions requires a multidimensional analysis that can account for the net behavior of the entire system. In fact, this concept is not new. In their widely read article on assessing mitochondrial function in cells, Nicholls and Brand highlighted the use of the respiratory control ratio (RCR) as a practical single parameter indicator of mitochondrial function, but also cautioned that a more detailed modular analysis should be performed to avoid ambiguity in the interpretation of RCRs (47).

One of the most prevalent limitations in the interpretation of bioenergetics studies is that mitochondrial functional parameters are measured under extreme assay conditions that (by design) elicit large effects. For example, maximal state 3 or state 4 respiration is often used in conjunction with SUIIT strategies to identify rate or energetically limiting steps in OxPhos. These measurements are then interpreted as a diagnosis of respiratory complex deficiency or more broad mitochondrial limitation and/or dysfunction. However, this logic is flawed both conceptually and experimentally. Conceptually, a limitation measured at capacity is only relevant if the physiological system reaches that capacity, which is rarely (if ever) demonstrated. Additionally, measurements made under extreme assay conditions do not inform the potential limitations of a system functioning below maximal capacity, which more closely represents the physiological state of cells. From an experimental perspective, the conditions in which typical SUIIT strategies are performed include: 1) saturated substrate transport (potentially superseding carrier mediated transport), 2) collapsed membrane potential induced by saturating ADP or uncoupling agents, and 3) adenylate mass action ratios that are opposite to those that occur in live cells, which likely understates the importance of thermodynamic and allosteric control mechanisms (53, 69, 168). These SUIIT strategies have been time tested and are useful but were explicitly developed to interrogate the mechanisms that underlie OxPhos, not to investigate the complex roles that OxPhos and other energy-linked processes play in cellular physiology. To accomplish the latter, new iterative testable models derived from multiplexed measurements in both intact cells and IM/PCs must be developed.

Intact cells

The most common EFA assay applied to intact cells is sometimes referred to as a "mito stress test" and is comprised of oxygen consumption rate measurement combined with a brief SUIIT protocol from which several parameters are often calculated including: basal, ATP linked, non-ATP linked (leak), uncoupled (reserve), and nonmitochondrial respiration (47). This design evolved from several decades of work in isolated mitochondria aimed at determining the net coupling stoichiometry between respiration in the ETS and ADP phosphorylation (8, 22, 23, 47). There are, however, several important considerations that can influence the interpretation of this assay and its individual parameters (Fig. 3). First, different net substrate oxidation patterns can exhibit different rates of respiration in support of the same power output (Box 1) and

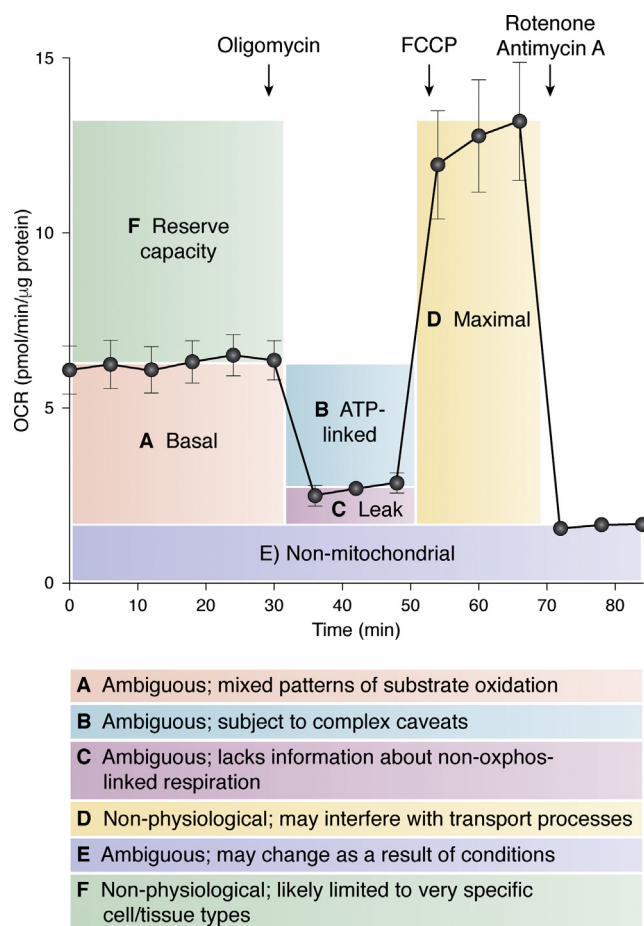


Figure 3. Ambiguities and other considerations involved in interpretation of the popular "mito stress test" respirometry assay and its related parameters.

are difficult to control in intact cells. Second, ATP-linked respiration is determined from additions of Oligomycin, but there are several complex caveats that impact the quality of this assumption (169). Third, the difference between uncoupled and basal respiration rates is often interpreted to be a measure of respiratory "reserve capacity" (83, 170). Though this may seem a reasonable interpretation, empirical correlation between uncoupled respiration rates and intact tissue respiratory reserve has not been demonstrated outside of very specific circumstances (e.g., in resting *versus* exercising skeletal muscle) (171, 172). The concept likely holds in skeletal muscle because myofibers undergo large changes in energy demand over short timescales during exercise. However, the extent to which this concept applies to other cell types or cells growing in subculture is not known. Finally, chemical uncoupling agents disrupt membrane transport processes that depend on voltage potential, which may result in a biased interpretation of substrate utilization due to confounding effects of these compounds alone (48). This assay design is indeed a good "starting point" and does provide some information regarding respiratory control by OxPhos. However, some of the measured and subsequently calculated parameters are limited by ambiguities or lack a clear physiological meaning (Fig. 3).

Force-flow analysis

Many of the limitations discussed above can be explored further using IM/PC preparations. For example: 1) Kinetic parameters involving specific substrate oxidation pathways can be more precisely assessed by isolating specific ETS-linked reactions (46), 2) OxPhos coupling can be targeted with other inhibitors such as carboxyatractyloside or bongkreikic acid (ATP/ADP carrier inhibitors) to provide additional resolution on the degree of coupling with OxPhos (43, 58), and 3) removing the plasma membrane barrier relieves some of the transport related ambiguity that occurs in intact cells. Despite these considerations, the lack of physiologically relevant adenylate ratios presents a major limitation to interpretation of these measurements due to the absence of normal energetic and allosteric regulatory mechanisms exerted by physiological ΔG_{ATP} . Additionally, $\Delta\Psi_m$ measurements can only be made under extreme states involving depolarization or hyperpolarization (*i.e.*, state 4 or state 3/u respectively), where this measurement has limited physiological relevance.

Fortunately, a collection of pioneering studies over the last few decades has led to the development of an elegant *in vitro* IM/PC-based system that utilizes purified creatine kinase enzyme to "clamp" the free ATP/ADP concentration ratio (and thus, ΔG_{ATP}) at fixed values by taking advantage of the known equilibrium constant of the reaction (K'_{CK}) (Fig. 4A) (41, 77, 173).

$$\Delta G_{ATP} = \Delta G'^{\circ}_{ATP} + RT \ln \left(\frac{[Creatine][Phosphate]}{[Phosphocreatine]K'_{CK}} \right) \quad (3)$$

This can be used to assess respiratory kinetics over a physiologically relevant range of phosphate potential values and allows unprecedented examination of the energetic-kinetic relationships that support OxPhos (34, 41). Another advantage of this system is that the phosphate potential can be increased (*i.e.*, more negative ΔG_{ATP} ; analogous to reduced cellular energetic demand) through the creatine kinase reaction equilibrium by titration of known amounts of phosphocreatine (Fig. 4, B and C) (34, 41, 77). This more closely models the *in vivo* control over respiration rate that is exerted over a physiological demand range (34, 41, 77, 174), resulting in concomitant reduction in steady-state respiratory flux described by the following relationship:

$$J_{O_2} = \sigma \Delta G_{ATP} \quad (4)$$

where σ is a phenomenological coefficient denoted "conductance" that is equal to the rate of change in flux (J_{O_2}) with respect to unit change in ΔG_{ATP} (34, 168). Conductance is the inverse of resistance, and as such, an observed change/difference in conductance among experimental groups implies that one or more source(s) of resistance in the mitochondrial energy transduction system (*i.e.*, the four control nodes) are responsible (Fig. 4D). It is important to note that the empirical relationship becomes nonlinear at extreme values of ΔG_{ATP} and the interpretation of this assay becomes complex. Thus, the conductance is best interpreted in the "linear" range of the curve and must be optimized for different tissue/cell types to

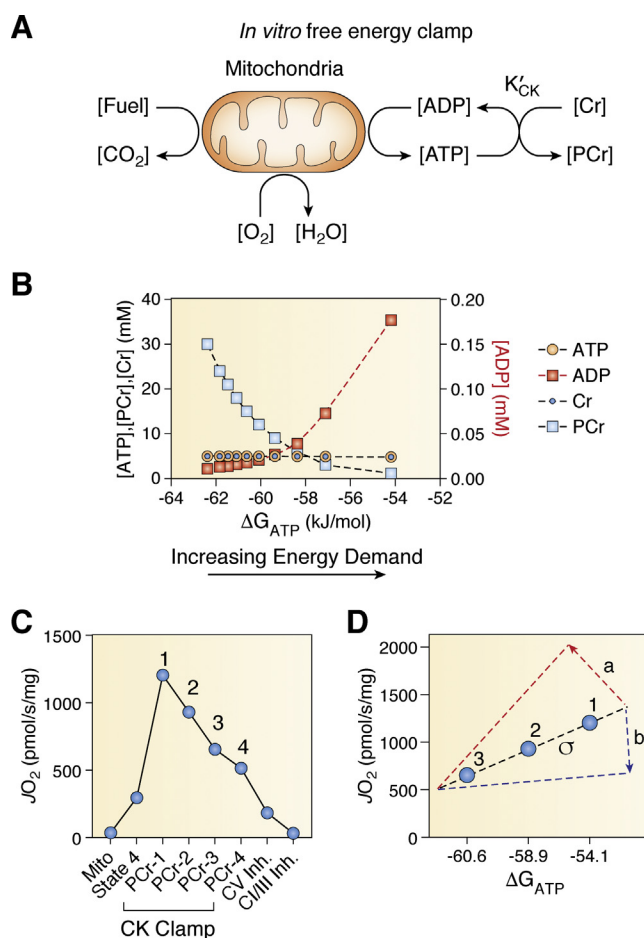


Figure 4. Creatine kinase (free energy) clamp system for assessing mitochondrial function in IM/PCs under a physiological range of ATP hydrolysis free energy (ΔG_{ATP}). A, diagram summarizing clamp concept. B, changes in ADP, ATP, Creatine, and Phosphocreatine concentrations versus resulting values of ΔG_{ATP} . More negative ΔG_{ATP} represents a lower energetic demand state. C, hypothetical example of a free energy clamp experiment using isolated mitochondria. PCr- Phosphocreatine; CV- Respiratory complex V (ATP synthase); CI/III- Complexes I and III respectively. D, representative conductance (σ) over the linear portion of the curve in subpanel C. An increase in slope (conductance) indicates greater control of flux by OxPhos (a), a decrease indicates lower control by OxPhos (b).

ensure that this is the case. Additionally, the free energy values are calculated from the assay conditions, which is not trivial. To aid researchers in designing and interpreting experiments, an open-source online calculator is available (Bioenergetic Calculators (dmpio.github.io)) (34).

The goal of force-flow analysis is to simultaneously account for the driving and driven energetic forces that influence the kinetics of mitochondrial respiration under conditions that more closely recapitulate the living cell. A change/difference in conductance implies alteration in the apparent coupling efficiency of OxPhos, which is also related to the ATP/O stoichiometry. The stoichiometries of proton translocation by the ETS and ATP synthase are generally considered to be fixed (though may vary by taxonomy) (22). Thus, the two most likely sources of variation in conductance in IM/PC preparations are derived from substrate oxidation stoichiometries (Box 1) or non-OxPhos coupled respiration. Though a change/difference in conductance does

not indicate the specific source of altered "efficiency," this can be further investigated by including additional measurements (34).

The $\Delta\Psi_m$ (energy intermediate) node is proportional to the mitochondrial proton motive force. Importantly, $\Delta\Psi_m$ has complex properties that should be considered when measuring this variable (highlighted in Box 2). $\Delta\Psi_m$ is typically measured using cationic indicators (fluorescent or potentiometric), which have many uses/interpretations depending on the preparation type and context (47, 134, 175). Quantitatively monitoring $\Delta\Psi_m$ can be a complicated business (133, 176). However, it can be made slightly less complicated (albeit at a cost to accuracy) by making a few simplifying assumptions and fluorescence can be calibrated using described methods (34, 177). Note that cationic indicators often affect respiration rates and should be included uniformly across replicates/conditions

Box 2. Mitochondrial membrane potential and proton motive force

The principal function of the mitochondrial pmf is to facilitate the energetically favorable transfer of molecules across the selectively permeable inner membrane. As discussed in Box 1, pmf is a form of energy intermediate derived from the ΔG of the redox spans from the various electron carriers to oxygen. The highly directional suite of transport processes that depend on pmf are linked to critical mitochondrial and greater cellular functions including protein import (219), ADP phosphorylation (220), control of cytosolic and matrix redox states (110, 112, 221), and metabolite interconversion (54). The pmf is derived from the proton pumping activities of NADH:ubiquinone oxidoreductase (Complex I), CoQ:cytochrome c oxidoreductase (Complex III), and Cytochrome c oxidase (Complex IV) (128, 222). The pmf can be stated compactly as:

$$\text{pmf} = F\Delta\Psi_m + 2.3RT\Delta\text{pH} \quad (1)$$

where $\Delta\Psi_m = \Psi_{\text{matrix}} - \Psi_{\text{cytosol}}$ and $\Delta\text{pH} = \text{pH}_{\text{matrix}} - \text{pH}_{\text{cytosol}}$. The constant (2.3) converts the natural logarithm that is classically used in this expression to base 10, which is the scale on which pH is represented. F is Faraday's constant, and R and T are the ideal gas constant and absolute temperature, respectively. F is Faraday's constant, and R and T are the ideal gas constant and absolute temperature, respectively. The pmf is an expression of an electrochemical potential and is comprised of both the voltage potential difference ($\Delta\Psi_m$) and the proton concentration gradient (ΔpH). Importantly, the $\Delta\Psi_m$ component is a manifestation of the balance of all charged species that equilibrate in response to changes in ΔpH (e.g., K^+ , Na^+ , Ca^{2+} , Mg^{2+} , HPO_4^{2-} , organic acids, etc) (202). In animal cells, $\Delta\Psi_m$ generally makes a larger energetic contribution to the steady-state pmf value compared with ΔpH (approx. -150 mV versus -50 mV respectively) (132, 176). Changes in each term can relate to distinct physical consequences. For example, transport of cations into the matrix (or anions out) is energetically dependent on the magnitude of the $\Delta\Psi_m$ term (54, 110, 223), while processes that directly transfer protons into the matrix such as ADP phosphorylation by ATP synthase are kinetically and energetically dependent on the magnitude of ΔpH (224). Additionally, many carbon substrates of the TCA cycle and other pathways are weak acids (i.e., ionize at different pH values), and their distribution is dependent on magnitude of both $\Delta\Psi_m$ and ΔpH (54). Notably, $\Delta\Psi_m$ is framed in reference to only one ionic species (H^+), because it is actively produced by proton pumping, and all other permeant ions are considered to equilibrate with the diffusive and electrical forces through passive or secondary-active transport processes (54, 128, 202). For this reason, it is important that the net ion current can be reasonably assumed to be zero during experimental determination of $\Delta\Psi_m$ (i.e., no change in net ion concentrations across the membrane over time). During steady-state respiration, this is taken to be the case. However, if such a steady state cannot be achieved, then permeabilities of other ions may contribute significantly to the $\Delta\Psi_m$ requiring use of the Goldman-Hodgkin-Katz relation (225). Though changes in mitochondrial membrane potential are often reported in conjunction with pathological states, such results must be interpreted cautiously. The membrane potential is a function of both energy "supply" and "demand" and small changes may reflect large kinetic responses. For these reasons, measurements of membrane potential alone are insufficient to define mitochondrial function.

at the lowest concentrations that achieve the desired effects (with additional attention paid the importance of dye quenching) (177, 178). Additionally, cationic indicators should not be used without accompanying respiration experiments to account for potential inhibitory or uncoupling effects that are quite common among these molecules. When appropriately measured, $\Delta\Psi_m$ is useful because it provides information about the balance between energy supply and demand. When the third node (demand) is fixed under free energy clamped conditions (Fig. 5A), $\Delta\Psi_m$ becomes proportional to the input force and the relationships among energetics and kinetics (i.e., force flow) can be compared among experimental groups/conditions. A leftward shift (more negative/polarized state) in $\Delta\Psi_m$ at the same conductance implies increased coupling efficiency of OxPhos (Fig. 5B). A rightward shift in $\Delta\Psi_m$ (less negative/depolarized state) at the same conductance implies reduced coupling efficiency of OxPhos (i.e., physiological or nonphysiological uncoupling) or may result from rate limitations in the ETS or substrate oxidation nodes (Fig. 5B).

Changes in the input forces (i.e., the substrate oxidation node) can be difficult to quantify. However, under controlled conditions, the fractional reduction of the pyridine nucleotide pool (NAD(P)H) can provide some additional qualitative information regarding the dehydrogenase reactions that support the ETS and can be measured using the autofluorescence of these molecules that is excited by long-wavelength UV light (34). This can be readily measured using a fluorometer or microtiter plate reader, and experimental conditions can be designed to determine the maximal/minimal reduced states via SUI assays (Fig. 5C). Notably, the NAD(P)H redox state may not change significantly over the clamped ΔG_{ATP} range in isolated mitochondria preparations due to the necessity of including saturating substrates, which by design causes the substrate oxidation node to be fully reduced. This effect may vary with the biological system/conditions under study, and a hyper-reduced state (Fig. 5D) may indicate specific respiratory complex deficiencies as the primary mode of resistance becomes the ETS. This effect has been demonstrated in heart mitochondria of mice with compromised DNA repair (162). A more oxidized state (Fig. 5D) may indicate a limitation imposed by specific dehydrogenase expression or activities, or uncoupling mechanisms that can each be investigated with other methods (34).

Finally, ADP phosphorylation rate is often interpolated from respiration rates due the presumed tightly coupled nature or these processes, but the degree of OxPhos coupling may change under different conditions. Thus, an additional method that empirically measures the ADP phosphorylation rate can be useful for further investigating observed changes/differences in conductance. This can be accomplished in IM/PC preparations using hexokinase clamped ATP hydrolysis with glucose-6-phosphate dehydrogenase linked NADPH autofluorescence in the presence of respiring mitochondria to empirically determine OxPhos rates in real time (76). When measured in parallel with JO_2 under matched conditions, this method can be used to empirically determine ATP/O stoichiometry, and the causes of apparent discrepancy between

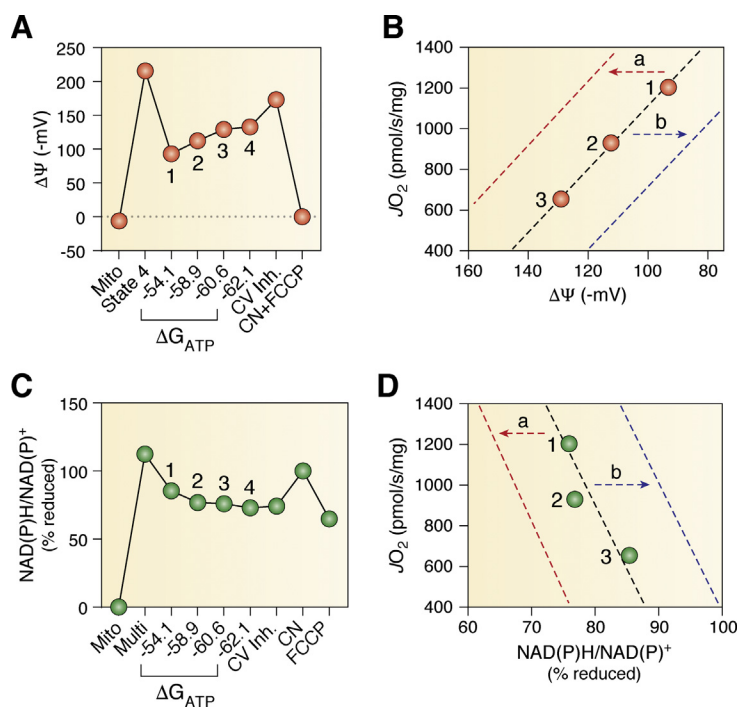


Figure 5. Force-flow analysis for additional investigation of mitochondrial energy transduction. A, hypothetical experiment demonstrating inner mitochondrial membrane potential ($\Delta\Psi_m$) via quench mode TMRM measured under CK clamp conditions using isolated mitochondria. CN- Potassium Cyanide. Numbers indicate chronological order of PCR addition. B, a decrease in $\Delta\Psi_m$ with unchanged conductance indicates reduced OxPhos coupling efficiency or limitations in the energy supply node (a). An increase in $\Delta\Psi_m$ with unchanged conductance indicates increased OxPhos coupling efficiency or rate limitation by respiratory complex V (b). C, hypothetical experiment for qualitative assessment of the redox state of the substrate oxidation node under CK clamp conditions using isolated mitochondria. D, a decrease in % reduced with unchanged conductance indicates reduced OxPhos coupling efficiency or limitations in the energy supply node (a). An increase in % reduced with unchanged conductance indicates increased OxPhos coupling efficiency or rate limitation by proton pumping complexes in the ETS (b).

measured and theoretical ATP/O ratios for the substrate conditions can be further explored using other methods (22, 34). Importantly, the hexokinase enzymatic clamp system does not support physiological adenylate ratios (*i.e.*, ADP is much higher than ATP), but this is the best approach currently available. When this assay is performed in parallel with force-flow analysis, and ADP concentrations are carefully matched among the two experiments, all the parameters necessary to calculate power output to the phosphate potential are determined (as described in Box 1).

Respiration versus OxPhos and the efficiency of oxidative phosphorylation

As support for the chemiosmotic theory grew in the mid-20th century, many early studies were performed with the aim of determining mechanistic ATP/O ratios and were designed to minimize implications of ETS flux that was not linked to the phosphorylation of ADP (*i.e.*, uncoupled respiration) (22). Many of these early studies formed the basis of contemporary practices for assaying mitochondrial function, which have ultimately retained some of those design elements: *e.g.*, use of oligomycin, Ca²⁺ chelators, albumin, and buffer compositions optimized for high RCRs (23, 179). Due to the popularity of the "mito stress test" assay (Fig. 3), the apparent coupling efficiency of OxPhos has now been determined for a wide variety of cultured cell types under various substrate supported conditions. A brief survey of representative data for

several distinct cell types indicates that astonishing variation (40–90%) in coupling efficiency is quite common (180–184). This demonstrates that, in some cell types/conditions, most of the respiration may not be committed to supporting OxPhos. Though such conclusions could be met with skepticism due to the fact that media conditions may facilitate artifactual adaptations in central carbon metabolism (185, 186), observations of age-dependent reduction in ADP phosphorylation rate in the absence of change in J_{O_2} in mouse skeletal muscle *in vivo* provide further support for the complexity and physiologic relevance of OxPhos independent respiration (187–189).

In addition to the observations discussed above, several other recent studies have documented that mitochondrial flux may be more important than OxPhos under certain conditions implying that it is time to rethink the universality of the "powerhouse of the cell" anachronism (103, 104, 106, 190, 191). The putative role of physiological uncoupling of respiration from OxPhos is not well understood. It has been shown that less than 5% of basal proton leak is mediated by passive diffusion of protons through the lipid bilayer, suggesting that most of the uncoupling is mediated by inner membrane proteins and is probably tightly regulated (192). The expression of uncoupling proteins (UCPs) was first noted in brown adipose tissue and ascribed to a nonshivering thermogenic function (193, 194). The discovery of widespread UCP isoform expression in other cells/tissues and putative proton translocating activities of mitochondrial anion transporters of the SLC25 family suggests that processes other than

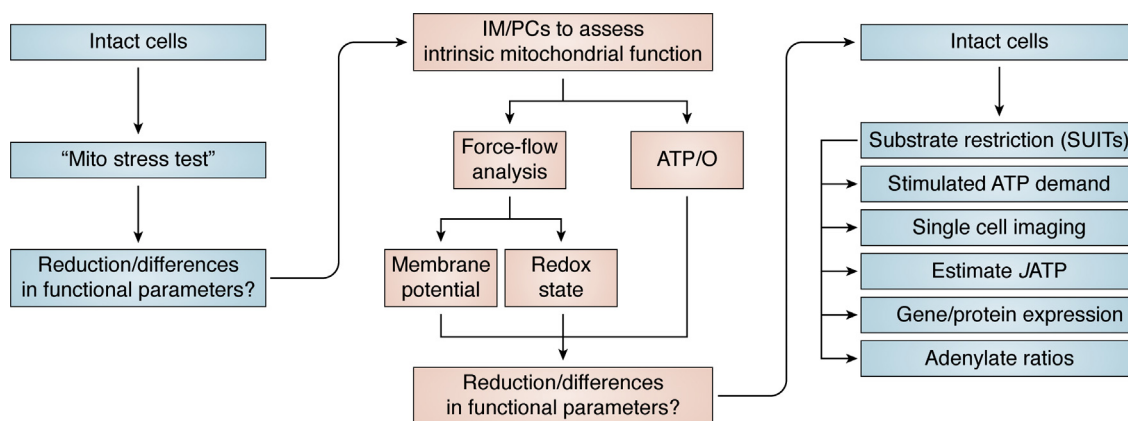


Figure 6. Representative workflow for reducing some of the ambiguity inherent in the "mito stress test" assay design by incorporating isolated mitochondria/permeabilized cells (IM/PC) data followed by further iterative testing in intact cells.

thermogenesis are also implicated in energy uncoupling (195–199). Another role of physiological uncoupling may be to facilitate increased TCA cycle flux in support of metabolite synthesis and exchange. For example, TCA cycle intermediates provide carbon backbones for nonessential amino acids and other anabolic reactions through cataplerosis (200, 201). Additionally, several well-characterized transport processes are electrogenic and are energetically dependent on $\Delta\Psi_m$ (54, 202, 203), and others depend on compensated proton symport (or as electroneutral protonated acids) and are thus dependent on the pH gradient component of $\Delta\Psi_m$ (54). A final mechanism of uncoupling worth mentioning is the prevention of oxidant stress *via* nicotinamide nucleotide transhydrogenase—an IMM protein that activates proton conductance to catalyze the resynthesis of NADPH needed to support flux through redox buffering circuits (32, 204).

Importantly, all of these processes are capable of contributing substantially to basal energy expenditure *in vivo*, but have been considered to make only a small contribution to respiration rate in isolated organelle experiments that have been classically focused on determining mechanistic ATP/O ratios (22). This is important because this view shades the way in which the physiological role of mitochondria within cells is framed, which is then echoed in the design of

bioenergetics experiments that typically focus on OxPhos. These factors must be considered as the field evolves to understand how mitochondria fit into the greater functionality of the cell, and it is clear that current assays must be expanded to include strategies that look beyond respiratory control exerted by OxPhos. Moving this idea forward will require approaches that can practically account for the coupling stoichiometry of OxPhos, and its relationship with non-OxPhos dependent mitochondrial respiration as it varies among cell types/conditions. The methods described in the previous section can be used to identify circumstances in which non-OxPhos coupled flux is occurring, but other approaches must be undertaken to identify the underlying causes.

Integration of intrinsic functional parameters with intact cell measurements

To reiterate, the IM/PC-based assays described in previous sections are intended to provide additional resolution on observations made in intact cells, with the ultimate goal of returning to the intact cells to test the new hypotheses (Fig. 6). To a limited degree, substrate oxidation patterns can be isolated in intact cells using strategic substrate deprivation/refeeding and appropriate inhibitors (31, 186). Under conditions in which specific pathways can be reasonably isolated, JATP can be estimated using theoretical ATP/O ratios, which can then be compared with JATP calculated from empirically derived ATP/O ratios. Gene/protein expression strategies can be undertaken to investigate underlying causes/consequences of specific metabolic patterns identified in the analysis and cell/tissue fractionation may aid in identifying intrinsic mitochondrial expression patterns (162, 205). Controlled increases in physiological demand state can be induced by using ionophores that selectively permeabilize plasma membranes to ions in the media (206–209). In many cells, ATP-dependent ion exchange in response to depolarization results in increased energy expenditure, which can be selectively investigated using SUITs (31, 108, 114). However, these experiments must be very carefully controlled (and optimized) using titration of ion transporter inhibitors to ensure

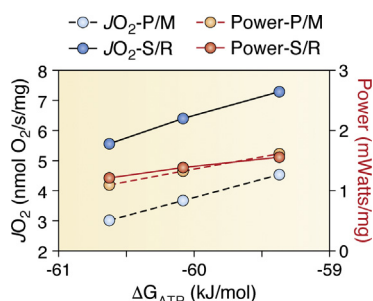


Figure 7. Coupling stoichiometry affects respiration rate required to maintain fixed power output. Creatine kinase (free energy) clamped respiration and power output to the phosphate potential calculated as described in Box 1 using previously published data obtained in isolated cardiac mitochondria from mouse heart (34). P/M, Pyruvate/Malate; S/R, Succinate/Rotenone.

specificity of the effect, and ionophore concentrations must be minimized because they are generally not membrane specific and may result in depolarization of the IMM in addition to the plasma membrane (176). Finally, quantitative imaging of potentiometric dyes can be extremely useful for investigating the importance of mitochondrial structure, content, and spatial distribution within cells and can also be performed under conditions that parallel other functional parameter measurements (31). This approach can also be used to assess whether mitochondrial structure/content is retained under permeabilizing conditions.

Conclusion

Bioenergetics assay design must account for minute changes in assay conditions as well as emphasize normalization and standardization due to the many factors that may independently introduce variability. Additionally, it may be time to rethink some of the historical assumptions that have shaded the view of bioenergetic organization, particularly with regard to the universality of the "textbook" model of glycolysis and oxidative phosphorylation and the ill-defined notion of mitochondrial "dysfunction." Bioenergetics research has been challenged historically by the reliance on extreme assay conditions that fail to recapitulate the balance of free energies (ΔG_{redox} , $\Delta G_{\Delta\Psi}$, ΔG_{ATP} , etc.) and the demand-driven nature under which the system operates *in vivo* to draw conclusions that are at best tenuously related to physiology. Improvements can be made on these approaches by leveraging recent advances in multiplexed assay design that unify information obtained in both intact cells as well as isolated mitochondria/permeabilized cells that ultimately culminate in iterative development of testable models in intact cells.

Finally, looking to the future, much of bioenergetics research has been focused on "metabolically active tissues and cell types" (*i.e.*, striated muscle, liver, pancreas, cancerous cells, etc). Perhaps the most promising progressive aim of bioenergetics research is simply the expansion of the collective understanding of the organization/regulation of cellular metabolism in cell types and biological contexts that have not yet been adequately studied. To achieve this, some of the assumptions regarding the canonical roles of metabolic systems must be cast off and assay design/interpretation must be afforded a measure of flexibility to accommodate unexpected observations. It is our hope that the concepts/approaches discussed in this review provide a modest starting point for such endeavors.

Author contributions—C. A. S., K. H. F.-W., and P. D. N., conceptualization; C. A. S., writing—original draft; C. A. S., K. H. F.-W., and P. D. N., writing—review and editing.

Funding and additional information—This work was supported by NIH NIDDK Award number F32DK127632 (C. A. S.), DoD-W81XWH-19-1-0213 (K. H. F.-W.), and NIH R01 AR071263, DK110656 and AG069679 (P. D. N.). The content is solely the

responsibility of the authors and does not necessarily represent the official views of the DoD or NIH.

Conflict of interest—The authors declare that they have no conflicts of interest with the contents of this article.

Abbreviations—The abbreviations used are: ECAR, extracellular acidification rate; EFA, extracellular flux analysis; ETS, electron transfer system; FAO, fatty acid oxidation; MAS, malate-aspartate shuttle; MFA, metabolic flux analysis; MPC, metal-porphyrin complex; OCR, oxygen consumption rate; OxPhos, oxidative phosphorylation; pmf, proton motive force; RCR, respiratory control ratio; ROS, reactive oxygen species; SUIT, substrate-inhibitor titration.

References

1. Jucker, M. (2010) The benefits and limitations of animal models for translational research in neurodegenerative diseases. *Nat. Med.* **16**, 1210–1214
2. Ruggeri, B. A., Camp, F., and Miknyoczki, S. (2014) Animal models of disease: Pre-clinical animal models of cancer and their applications and utility in drug discovery. *Biochem. Pharmacol.* **87**, 150–161
3. King, A. J. F. (2012) The use of animal models in diabetes research. *Br. J. Pharmacol.* **166**, 877–894
4. Cheng, Z., Tseng, Y., and White, M. F. (2010) Insulin signaling meets mitochondria in metabolism. *Trends Endocrinol. Metab.* **21**, 589–598
5. Nagarajan, A., Malvi, P., and Wajapeyee, N. (2016) Oncogene-directed alterations in cancer cell metabolism. *Trends Cancer* **2**, 365–377
6. Gao, C., Wang, Q., Chung, S. K., and Shen, J. (2017) Crosstalk of metabolic factors and neurogenic signaling in adult neurogenesis: Implication of metabolic regulation for mental and neurological diseases. *Neurochem. Int.* **106**, 24–36
7. Reily, C., Mitchell, T., Chacko, B. K., Benavides, G. A., Murphy, M. P., and Darley-Usmar, V. M. (2013) Mitochondrially targeted compounds and their impact on cellular bioenergetics. *Redox Biol.* **1**, 86–93
8. Gerencser, A. A., Neilson, A., Choi, S. W., Edman, U., Yadava, N., Oh, R. J., Ferrick, D. A., Nicholls, D. G., and Brand, M. D. (2009) Quantitative microplate-based respirometry with correction for oxygen diffusion. *Anal. Chem.* **81**, 6868–6878
9. Mookerjee, S. A., Goncalves, R. L. S., Gerencser, A. A., Nicholls, D. G., and Brand, M. D. (2015) The contributions of respiration and glycolysis to extracellular acid production. *Biochim. Biophys. Acta* **1847**, 171–181
10. Mookerjee, S. A., Gerencser, A. A., Nicholls, D. G., and Brand, M. D. (2017) Quantifying intracellular rates of glycolytic and oxidative ATP production and consumption using extracellular flux measurements. *J. Biol. Chem.* **292**, 7189–7207
11. Rana, P., Aleo, M. D., Gosink, M., and Will, Y. (2019) Evaluation of *in vitro* mitochondrial toxicity assays and physicochemical properties for prediction of organ toxicity using 228 pharmaceutical drugs. *Chem. Res. Toxicol.* **32**, 156–167
12. Gohil, V. M., Sheth, S. A., Nilsson, R., Wojtovich, A. P., Lee, J. H., Perocchi, F., Chen, W., Clish, C. B., Ayata, C., Brookes, P. S., and Mootha, V. K. (2010) Nutrient-sensitized screening for drugs that shift energy metabolism from mitochondrial respiration to glycolysis. *Nat. Biotechnol.* **28**, 249–255
13. Wu, M., Neilson, A., Swift, A. L., Moran, R., Tamagnine, J., Parslow, D., Armistead, S., Lemire, K., Orrell, J., Teich, J., Chomicz, S., and Ferrick, D. A. (2007) Multiparameter metabolic analysis reveals a close link between attenuated mitochondrial bioenergetic function and enhanced glycolysis dependency in human tumor cells. *Am. J. Physiol. Cell Physiol.* **292**, 125–136
14. Martin, S. D., and McGee, S. L. (2019) A systematic flux analysis approach to identify metabolic vulnerabilities in human breast cancer cell lines. *Cancer Metab.* **7**, 12

15. Dier, U., Shin, D. H., Madhubhani, L. P., Hemachandra, P., Uusitalo, L. M., and Hempel, N. (2014) Bioenergetic analysis of ovarian cancer cell lines: Profiling of histological subtypes and identification of a mitochondria-defective cell line. *PLoS One* **9**, e98479
16. Robinson, G. L., Dinsdale, D., MacFarlane, M., and Cain, K. (2012) Switching from aerobic glycolysis to oxidative phosphorylation modulates the sensitivity of mantle cell lymphoma cells to TRAIL. *Oncogene* **31**, 4996–5006
17. DeBerardinis, R. J., and Chandel, N. S. (2020) We need to talk about the Warburg effect. *Nat. Metab.* **2**, 127–129
18. Muoio, D. M., and Neuffer, P. D. (2012) Lipid-induced mitochondrial stress and insulin action in muscle. *Cell Metab.* **15**, 595–605
19. Wiechert, W. (2001) ¹³C metabolic flux analysis. *Metab. Eng.* **3**, 195–206
20. Antoniewicz, M. R. (2018) A guide to ¹³C metabolic flux analysis for the cancer biologist. *Exp. Mol. Med.* **50**, 1–13
21. Chance, B., and Williams, G. R. (1955) A simple and rapid assay of oxidative phosphorylation. *Nature* **175**, 1120–1121
22. Hinkle, P. C. (2005) P/O ratios of mitochondrial oxidative phosphorylation. *Biochim. Biophys. Acta* **1706**, 1–11
23. Chance, B., and Williams, G. R. (1956) The respiratory chain and oxidative phosphorylation. *Adv. Enzymol. Relat. Subj. Biochem.* **17**, 65–134
24. O'Donovan, C., Hynes, J., Yashunski, D., and Papkovsky, D. B. (2005) Phosphorescent oxygen-sensitive materials for biological applications. *J. Mater. Chem.* **15**, 2946–2951
25. Zhdanov, A. V., Ogurtsov, V. I., Taylor, C. T., and Papkovsky, D. B. (2010) Monitoring of cell oxygenation and responses to metabolic stimulation by intracellular oxygen sensing technique. *Integr. Biol. (Camb.)* **2**, 443–451
26. Haller, T., Ortner, M., and Gnaiger, E. (1994) A respirometer for investigating oxidative cell metabolism: Toward optimization of respiratory studies. *Anal. Biochem.* **218**, 338–342
27. Ripple, M. O., Kim, N., and Springett, R. (2013) Mammalian complex I pumps 4 protons per 2 electrons at high and physiological proton motive force in living cells. *J. Biol. Chem.* **288**, 5374–5380
28. Zhdanov, A. V., Favre, C., O'Flaherty, L., Adam, J., O'Connor, R., Pollard, P. J., and Papkovsky, D. B. (2011) Comparative bioenergetic assessment of transformed cells using a cell energy budget platform. *Integr. Biol. (Camb.)* **3**, 1135–1142
29. O'Riordan, T. C., Zhdanov, A. V., Ponomarev, G. V., and Papkovsky, D. B. (2007) Analysis of intracellular oxygen and metabolic responses of mammalian cells by time-resolved fluorometry. *Anal. Chem.* **79**, 9414–9419
30. Hynes, J., O'Riordan, T. C., Zhdanov, A. V., Uray, G., Will, Y., and Papkovsky, D. B. (2009) *In vitro* analysis of cell metabolism using a long-decay pH-sensitive lanthanide probe and extracellular acidification assay. *Anal. Biochem.* **390**, 21–28
31. Schmidt, C. A., McLaughlin, K. L., Boykov, I. N., Mojalagbe, R., Ranganathan, A., Buddo, K. A., Lin, C.-T., Fisher-Wellman, K. H., and Neuffer, P. D. (2021) Glycemic growth enhances carbohydrate metabolism and induces sensitivity to menadione in cultured tumor-derived cells. *Cancer Metab.* **9**, 1–21
32. Fisher-Wellman, K. H., Lin, C. T., Ryan, T. E., Reese, L. R., Gilliam, L. A. A., Cathey, B. L., Lark, D. S., Smith, C. D., Muoio, D. M., and Neuffer, P. D. (2015) Pyruvate dehydrogenase complex and nicotinamide nucleotide transhydrogenase constitute an energy-consuming redox circuit. *Biochem. J.* **467**, 271–280
33. Blacker, T. S., and Duchon, M. R. (2016) Investigating mitochondrial redox state using NADH and NADPH autofluorescence. *Free Radic. Biol. Med.* **100**, 53–65
34. Fisher-Wellman, K. H., Davidson, M. T., Narowski, T. M., Lin, C. T., Koves, T. R., and Muoio, D. M. (2018) Mitochondrial diagnostics: A multiplexed assay platform for comprehensive assessment of mitochondrial energy fluxes. *Cell Rep.* **24**, 3593–3606.e10
35. Takahashi, A., Zhang, Y., Centonze, V. E., and Herman, B. (2001) Measurement of mitochondrial pH *in situ*. *Biotechniques* **30**, 804–815
36. Roe, M. W., Lemasters, J. J., and Herman, B. (1990) Assessment of Fura-2 for measurements of cytosolic free calcium. *Cell Calcium* **11**, 63–73
37. Shirmanova, M. V., Druzhkova, I. N., Lukina, M. M., Matlashov, M. E., Belousov, V. V., Snopova, L. B., Prodanetz, N. N., Dudenkova, V. V., Lukyanov, S. A., and Zagaynova, E. V. (2015) Intracellular pH imaging in cancer cells *in vitro* and tumors *in vivo* using the new genetically encoded sensor SypHer2. *Biochim. Biophys. Acta* **1850**, 1905–1911
38. Fan, Y., Makar, M., Wang, M. X., and Ai, H. (2017) Monitoring thio-redoxin redox with a genetically encoded red fluorescent biosensor. *Nat. Chem. Biol.* **13**, 1045–1052
39. Tao, R., Zhao, Y., Chu, H., Wang, A., Zhu, J., Chen, X., Zou, Y., Shi, M., Liu, R., Su, N., Du, J., Zhou, H.-M., Zhu, L., Qian, X., Liu, H., *et al.* (2017) Genetically encoded fluorescent sensors reveal dynamic regulation of NADPH metabolism. *Nat. Methods* **14**, 720–728
40. Bradshaw, P. C., and Pfeiffer, D. R. (2006) Release of Ca²⁺ and Mg²⁺ from yeast mitochondria is stimulated by increased ionic strength. *BMC Biochem.* **7**, 1–12
41. Glancy, B., Willis, W. T., Chess, D. J., and Balaban, R. S. (2013) Effect of calcium on the oxidative phosphorylation cascade in skeletal muscle mitochondria. *Biochemistry* **52**, 2793–2809
42. Golding, E. M., Teague, W. E., and Dobson, G. P. (1995) Adjustment of K⁺ to varying pH and pMg for the creatine kinase, adenylate kinase and ATP hydrolysis equilibria permitting quantitative bioenergetic assessment. *J. Exp. Biol.* **198**, 1775–1782
43. Nicholls, D., and Ferguson, S. (2013) *Bioenergetics*, 4th Ed, Academic Press, London, UK
44. Gnaiger, E. (2020) *Mitochondrial Pathways and Respiratory Control: An Introduction to OXPHOS Analysis*, 5th Ed., Bioenergetics Communications, Innsbruck, Austria
45. Kacser, H., Burns, J. A., and Fell, D. A. (1995) The control of flux: 21 years on. *Biochem. Soc. Trans.* **23**, 341–366
46. Perry, C. G. R., Kane, D. A., Lanza, I. R., and Neuffer, P. D. (2013) Methods for assessing mitochondrial function in diabetes. *Diabetes* **62**, 1041–1053
47. Brand, M. D., and Nicholls, D. G. (2011) Assessing mitochondrial dysfunction in cells. *Biochem. J.* **435**, 297–312
48. Wollenman, L. C., Vander Ploeg, M. R., Miller, M. L., Zhang, Y., and Bazil, J. N. (2017) The effect of respiration buffer composition on mitochondrial metabolism and function. *PLoS One* **12**, e0187523
49. Jaber, S. M., Yadava, N., and Polster, B. M. (2020) Mapping mitochondrial respiratory chain deficiencies by respirometry: Beyond the Mito Stress Test. *Exp. Neurol.* **328**, 113282
50. Makrecka-Kuka, M., Krumschnabel, G., and Gnaiger, E. (2015) High-resolution respirometry for simultaneous measurement of oxygen and hydrogen peroxide fluxes in permeabilized cells, tissue homogenate and isolated mitochondria. *Biomolecules* **5**, 1319–1338
51. Halestrap, A. P., and Wilson, M. C. (2012) The monocarboxylate transporter family-role and regulation. *IUBMB Life* **64**, 109–119
52. McCommis, K., and Finck, B. (2015) Mitochondrial pyruvate transport: A historical perspective and future research directions. *Biochem. J.* **466**, 443–454
53. Edlund, G. L., and Halestrap, A. P. (1988) The kinetics of transport of lactate and pyruvate into rat hepatocytes. Evidence for the presence of a specific carrier similar to that in erythrocytes. *Biochem. J.* **249**, 117–126
54. LaNoue, K. F., and Schoolwerth, A. C. (1979) Metabolite transport in mitochondria. *Annu. Rev. Biochem.* **48**, 871–922
55. Vander Heiden, M. G., Plas, D. R., Rathmell, J. C., Fox, C. J., Harris, M. H., and Thompson, C. B. (2001) Growth factors can influence cell growth and survival through effects on glucose metabolism. *Mol. Cell. Biol.* **21**, 5899–5912
56. Xintaropoulou, C., Ward, C., Wise, A., Marston, H., Turnbull, A., and Langdon, S. P. (2015) A comparative analysis of inhibitors of the glycolysis pathway in breast and ovarian cancer cell line models. *Oncotarget* **6**, 25677–25695
57. Miyoshi, H. (1998) Structure-activity relationships of some complex I inhibitors. *Biochim. Biophys. Acta* **1364**, 236–244
58. Hong, S., and Pedersen, P. L. (2008) ATP synthase and the actions of inhibitors utilized to study its roles in human health, disease, and other scientific areas. *Microbiol. Mol. Biol. Rev.* **72**, 590–641

59. Smith, P. K., Krohn, R. I., Hermanson, G. T., Mallia, A. K., Gartner, F. H., Provenzano, M. D., Fujimoto, E. K., Goeke, N. M., Olson, B. J., and Klenk, D. C. (1985) Measurement of protein using bicinchoninic acid. *Anal. Biochem.* **150**, 76–85
60. McLaughlin, K. L., Hagen, J. T., Coalson, H. S., Nelson, M. A. M., Kew, K. A., Wooten, A. R., and Fisher-Wellman, K. H. (2020) Novel approach to quantify mitochondrial content and intrinsic bioenergetic efficiency across organs. *Sci. Rep.* **10**, 17599
61. Westheimer, F. H. (1987) Why nature chose phosphates. *Science* **235**, 1173–1178
62. Chen, Z., Zuo, X., Zhang, Y., Han, G., Zhang, L., Wu, J., and Wang, X. (2018) MiR-3662 suppresses hepatocellular carcinoma growth through inhibition of HIF-1 α -mediated Warburg effect. *Cell Death Dis.* **9**, 549
63. Kovalenko, I., Glasauer, A., Schöckel, L., Sauter, D. R. P., Ehrmann, A., Sohler, F., Hägebarth, A., Novak, I., and Christian, S. (2016) Identification of KCa 3.1 channel as a novel regulator of oxidative phosphorylation in a subset of pancreatic carcinoma cell lines. *PLoS One* **11**, e0160658
64. Wang, L., Yang, Q., Peng, S., and Liu, X. (2019) The combination of the glycolysis inhibitor 2-DG and sorafenib can be effective against sorafenib-tolerant persister cancer cells. *Oncol. Targets Ther.* **12**, 5359–5373
65. Calderwood, S. K., Bump, E. A., Stevenson, M. A., Van Kersen, I., and Hahn, G. M. (1985) Investigation of adenylate energy charge, phosphorylation potential, and ATP concentration in cells stressed with starvation and heat. *J. Cell. Physiol.* **124**, 261–268
66. Veech, R. L., Lawson, J. W., Cornell, N. W., and Krebs, H. A. (1979) Cytosolic phosphorylation potential. *J. Biol. Chem.* **254**, 6538–6547
67. Gnaiger, E. (1993) Nonequilibrium thermodynamics of energy transformations. *Pure Appl. Chem.* **65**, 1983–2002
68. Welch, G. R. (1985) Some problems in the usage of Gibbs free energy in biochemistry. *J. Theor. Biol.* **114**, 433–446
69. Alberty, R. A. (1968) Effect of pH and metal ion concentration on the equilibrium hydrolysis of adenosine triphosphate to adenosine diphosphate. *J. Biol. Chem.* **243**, 1337–1343
70. Furuhashi, M. (2020) New insights into purine metabolism in metabolic diseases: Role of xanthine oxidoreductase activity. *Am. J. Physiol. Endocrinol. Metab.* **319**, E827–E834
71. Atkinson, D. E., and Walton, G. M. (1967) Adenosine triphosphate conservation in metabolic regulation rat liver citrate cleavage enzyme. *J. Biol. Chem.* **242**, 3239–3241
72. Chapman, A. G., Fall, L., and Atkinson, D. E. (1971) Adenylate energy charge in *Escherichia coli* during growth and starvation. *J. Bacteriol.* **108**, 1072–1086
73. Brault, J. J., Pizzimenti, N. M., Dentel, J. N., and Wiseman, R. W. (2013) Selective inhibition of ATPase activity during contraction alters the activation of p38 MAP kinase isoforms in skeletal muscle. *J. Cell. Biochem.* **114**, 1445–1455
74. Glancy, B., and Balaban, R. S. (2021) Energy metabolism design of the striated muscle cell. *Physiol. Rev.* **101**, 1561–1607
75. Wiseman, R. W., and Kushmerick, M. J. (1995) Creatine kinase equilibrium follows solution thermodynamics in skeletal muscle: ³¹P NMR studies using creatine analogs. *J. Biol. Chem.* **270**, 12428–12438
76. Lark, D. S., Torres, M. J., Lin, C. T., Ryan, T. E., Anderson, E. J., and Neuffer, P. D. (2016) Direct real-time quantification of mitochondrial oxidative phosphorylation efficiency in permeabilized skeletal muscle myofibers. *Am. J. Physiol. Cell Physiol.* **311**, C239–C245
77. Messer, J. I., Jackman, M. R., and Willis, W. T. (2004) Pyruvate and citric acid cycle carbon requirements in isolated skeletal muscle mitochondria. *Am. J. Physiol. Cell Physiol.* **286**, C565–C572
78. Tanner, L. B., Goglia, A. G., Wei, M. H., Sehgal, T., Parsons, L. R., Park, J. O., White, E., Toettcher, J. E., and Rabinowitz, J. D. (2018) Four key steps control glycolytic flux in mammalian cells. *Cell Syst.* **7**, 49–62.e8
79. Park, J. O., Tanner, L. B., Wei, M. H., Khana, D. B., Jacobson, T. B., Zhang, Z., Rubin, S. A., Li, S. H. J., Higgins, M. B., Stevenson, D. M., Amador-Noguez, D., and Rabinowitz, J. D. (2019) Near-equilibrium glycolysis supports metabolic homeostasis and energy yield. *Nat. Chem. Biol.* **15**, 1001–1008
80. Xiao, Z., Dai, Z., and Locasale, J. W. (2019) Metabolic landscape of the tumor microenvironment at single cell resolution. *Nat. Commun.* **10**, 3763
81. Reitzer, L. J., Wice, B. M., and Kennell, D. (1979) Evidence that glutamine, not sugar, is the major energy source for cultured HeLa cells. *J. Biol. Chem.* **254**, 2669–2676
82. Hui, S., Ghergurovich, J. M., Morscher, R. J., Jang, C., Teng, X., Lu, W., Esparza, L. A., Reya, T., Zhan, L., Yanxiang Guo, J., White, E., and Rabinowitz, J. D. (2017) Glucose feeds the TCA cycle via circulating lactate. *Nature* **551**, 115–118
83. Perron, N. R., Beeson, C., and Rohrer, B. (2013) Early alterations in mitochondrial reserve capacity; a means to predict subsequent photoreceptor cell death. *J. Bioenerg. Biomembr.* **45**, 101–109
84. Hardie, R.-A., van Dam, E., Cowley, M., Han, T.-L., Balaban, S., Pajic, M., Pinese, M., Iconomou, M., Shearer, R. F., McKenna, J., Miller, D., Waddell, N., Pearson, J. V., Grimmond, S. M., Sazanov, L., et al. (2017) Mitochondrial mutations and metabolic adaptation in pancreatic cancer. *Cancer Metab.* **5**, 1–15
85. Keuper, M., Berti, L., Raedle, B., Sachs, S., Böhm, A., Fritsche, L., Fritsche, A., Häring, H. U., Hrabě de Angelis, M., Jastroch, M., Hofmann, S. M., and Staiger, H. (2019) Preadipocytes of obese humans display gender-specific bioenergetic responses to glucose and insulin. *Mol. Metab.* **20**, 28–37
86. Vijayan, V., Pradhan, P., Braud, L., Fuchs, H. R., Gueler, F., Motterlini, R., Foresti, R., and Immenschuh, S. (2019) Human and murine macrophages exhibit differential metabolic responses to lipopolysaccharide - a divergent role for glycolysis. *Redox Biol.* **22**, 101147
87. Warburg, O., Franz, W., and Negelein, E. (1927) The metabolism of tumours in the body. *J. Gen. Physiol.* **8**, 519–530
88. Warburg, O. (1956) On the origin of cancer cells. *Science* **123**, 309–314
89. Cassim, S., Vučetić, M., Ždraljević, M., and Pouyssegur, J. (2020) Warburg and beyond: The power of mitochondrial metabolism to collaborate or replace fermentative glycolysis in cancer. *Cancers (Basel)* **12**, 13–15
90. Morandi, A., and Indraccolo, S. (2017) Linking metabolic reprogramming to therapy resistance in cancer. *Biochim. Biophys. Acta Rev. Cancer* **1868**, 1–6
91. Handel, M. E., Brand, M. D., and Mookerjee, S. A. (2019) The whys and hows of calculating total cellular ATP production rate. *Trends Endocrinol. Metab.* **30**, 412–416
92. Bar-Even, A., Flamholz, A., Noor, E., and Milo, R. (2012) Rethinking glycolysis: On the biochemical logic of metabolic pathways. *Nat. Chem. Biol.* **8**, 509–517
93. Minakami, S., and Yoshikawa, H. (1966) Studies on erythrocyte glycolysis II. Free energy changes and rate limiting steps in erythrocyte glycolysis. *J. Biochem.* **59**, 139–144
94. Xie, J., Dai, C., and Hu, X. (2016) Evidence that does not support pyruvate kinase M2 (PKM2) - catalyzed reaction as a rate-limiting step in cancer cell glycolysis. *J. Biol. Chem.* **291**, 8987–8999
95. King, M. P., and Attardi, G. (1989) Human cells lacking mtDNA: Repopulation with exogenous mitochondria by complementation. *Science* **246**, 500–503
96. Alston, C. L., Rocha, M. C., Lax, N. Z., Turnbull, D. M., and Taylor, R. W. (2017) The genetics and pathology of mitochondrial disease. *J. Pathol.* **241**, 236–250
97. Johnson, D. T., Harris, R. A., Blair, P. V., and Balaban, R. S. (2007) Functional consequences of mitochondrial proteome heterogeneity. *Am. J. Physiol. Cell Physiol.* **292**, 698–707
98. Johnson, D. T., Harris, R. A., French, S., Blair, P. V., You, J., Bemis, K. G., Wang, M., and Balaban, R. S. (2007) Tissue heterogeneity of the mammalian mitochondrial proteome. *Am. J. Physiol. Cell Physiol.* **292**, 689–697
99. Konarzewski, M., and Książek, A. (2013) Determinants of intra-specific variation in basal metabolic rate. *J. Comp. Physiol. B* **183**, 27–41
100. Zhu, Z., Wang, Z., Zhang, C., Wang, Y., Zhang, H., Gan, Z., Guo, Z., and Wang, X. (2019) Mitochondrion-targeted platinum complexes suppressing lung cancer through multiple pathways involving energy metabolism. *Chem. Sci.* **10**, 3089–3095

101. O'Neill, S., Porter, R. K., McNamee, N., Martinez, V. G., and O'Driscoll, L. (2019) 2-Deoxy-D-glucose inhibits aggressive triple-negative breast cancer by targeting glycolysis and the cancer stem cell phenotype. *Sci. Rep.* **9**, 3788
102. Luengo, A., Li, Z., Gui, D. Y., Sullivan, L. B., Zagorulya, M., Do, B. T., Ferreira, R., Naamati, A., Ali, A., Lewis, C. A., Thomas, C. J., Spranger, S., Matheson, N. J., and Vander Heiden, M. G. (2021) Increased demand for NAD⁺ relative to ATP drives aerobic glycolysis. *Mol. Cell* **81**, 691–707.e6
103. Martínez-Reyes, I., Cardona, L. R., Kong, H., Vasan, K., McElroy, G. S., Werner, M., Kihshen, H., Reczek, C. R., Weinberg, S. E., Gao, P., Steinert, E. M., Piseaux, R., Budinger, G. R. S., and Chandel, N. S. (2020) Mitochondrial ubiquinol oxidation is necessary for tumour growth. *Nature* **585**, 288–292
104. Cardaci, S., Zheng, L., Mackay, G., Van Den Broek, N. J. F., Mackenzie, E. D., Nixon, C., Stevenson, D., Tumanov, S., Bulusu, V., Kamphorst, J. J., Vazquez, A., Fleming, S., Schiavi, F., Kalna, G., Blyth, K., *et al.* (2015) Pyruvate carboxylation enables growth of SDH-deficient cells by supporting aspartate biosynthesis. *Nat. Cell Biol.* **17**, 1317–1326
105. Fan, J., Kamphorst, J. J., Mathew, R., Chung, M. K., White, E., Shlomi, T., and Rabinowitz, J. D. (2013) Glutamine-driven oxidative phosphorylation is a major ATP source in transformed mammalian cells in both normoxia and hypoxia. *Mol. Syst. Biol.* **9**, 1–11
106. Mullen, A. R., Wheaton, W. W., Jin, E. S., Chen, P. H., Sullivan, L. B., Cheng, T., Yang, Y., Linehan, W. M., Chandel, N. S., and DeBerardinis, R. J. (2012) Reductive carboxylation supports growth in tumour cells with defective mitochondria. *Nature* **481**, 385–388
107. Yang, C., Ko, B., Hensley, C. T., Jiang, L., Wasti, A. T., Kim, J., Sudderth, J., Calvaruso, M. A., Lumata, L., Mitsche, M., Rutter, J., Merritt, M. E., and DeBerardinis, R. J. (2014) Glutamine oxidation maintains the TCA cycle and cell survival during impaired mitochondrial pyruvate transport. *Mol. Cell* **56**, 414–424
108. Epstein, T., Xu, L., Gillies, R. J., and Gatenby, R. A. (2014) Separation of metabolic supply and demand: Aerobic glycolysis as a normal physiological response to fluctuating energetic demands in the membrane. *Cancer Metab.* **2**, 7
109. Jang, S. R., Nelson, J. C., Bend, E. G., Rodríguez-Laureano, L., Tueros, F. G., Cartagena, L., Underwood, K., Jorgensen, E. M., and Colón-Ramos, D. A. (2016) Glycolytic enzymes localize to synapses under energy stress to support synaptic function. *Neuron* **90**, 278–291
110. Davis, E. J., Bremer, J., and Akerman, K. E. (1980) Thermodynamic aspects of translocation of reducing equivalents by mitochondria. *J. Biol. Chem.* **255**, 2277–2283
111. Glancy, B., Kane, D. A., Kavazis, A. N., Goodwin, M. L., Willis, W. T., and Gladden, L. B. (2021) Mitochondrial lactate metabolism: History and implications for exercise and disease. *J. Physiol.* **599**, 863–888
112. Barron, J. T., Gu, L., and Parrillo, J. E. (1998) Malate-aspartate shuttle, cytoplasmic NADH redox potential, and energetics in vascular smooth muscle. *J. Mol. Cell. Cardiol.* **30**, 1571–1579
113. Birsoy, K., Wang, T., Chen, W. W., Freinkman, E., Abu-Remaileh, M., and Sabatini, D. M. (2015) An essential role of the mitochondrial electron transport chain in cell proliferation is to enable aspartate synthesis. *Cell* **162**, 540–551
114. Mookerjee, S. A., Nicholls, D. G., and Brand, M. D. (2016) Determining maximum glycolytic capacity using extracellular flux measurements. *PLoS One* **11**, e0152016
115. Psychogios, N., Hau, D. D., Peng, J., Guo, A. C., Mandal, R., Bouatra, S., Sinelnikov, I., Krishnamurthy, R., Eisner, R., Gautam, B., Young, N., Xia, J., Knox, C., Dong, E., Huang, P., *et al.* (2011) The human serum metabolome. *PLoS One* **6**, e16957
116. Herbst, E. A. F., George, M. A. J., Brebner, K., Holloway, G. P., and Kane, D. A. (2018) Lactate is oxidized outside of the mitochondrial matrix in rodent brain. *Appl. Physiol. Nutr. Metab.* **43**, 467–474
117. Faubert, B., Li, K. Y., Cai, L., Hensley, C. T., Kim, J., Zacharias, L. G., Yang, C., Do, Q. N., Doucette, S., Burguete, D., Li, H., Huet, G., Yuan, Q., Wigal, T., Butt, Y., *et al.* (2017) Lactate metabolism in human lung tumors. *Cell* **171**, 358–371.e9
118. Young, A., Oldford, C., and Mailloux, R. J. (2020) Lactate dehydrogenase supports lactate oxidation in mitochondria isolated from different mouse tissues. *Redox Biol.* **28**, 101339
119. Prabhu, A. V., Krycer, J. R., and Brown, A. J. (2013) Overexpression of a key regulator of lipid homeostasis, Scap, promotes respiration in prostate cancer cells. *FEBS Lett.* **587**, 983–988
120. Hereng, T. H., Elgstøen, K. B. P., Cederkvist, F. H., Eide, L., Jahnsen, T., Sklhegg, B. S., and Rosendal, K. R. (2011) Exogenous pyruvate accelerates glycolysis and promotes capacitation in human spermatozoa. *Hum. Reprod.* **26**, 3249–3263
121. Owicki, J. C., and Wallace Parce, J. (1992) Biosensors based on the energy metabolism of living cells: The physical chemistry and cell biology of extracellular acidification. *Biosens. Bioelectron.* **7**, 255–272
122. Orlenko, A., Hermansen, R. A., and Liberles, D. A. (2016) Flux control in glycolysis varies across the tree of life. *J. Mol. Evol.* **82**, 146–161
123. Ainscow, E. K., and Brand, M. D. (1999) Internal regulation of ATP turnover, glycolysis and oxidative phosphorylation in rat hepatocytes. *Eur. J. Biochem.* **266**, 737–749
124. Shestov, A. A., Liu, X., Ser, Z., Cluntun, A. A., Hung, Y. P., Huang, L., Kim, D., Le, A., Yellen, G., Albeck, J. G., and Locasale, J. W. (2014) Quantitative determinants of aerobic glycolysis identify flux through the enzyme GAPDH as a limiting step. *Elife* **3**, e03342
125. Altinok, O., Poggio, J. L., Stein, D. E., Bowne, W. B., Shieh, A. C., Snyder, N. W., and Orynbayeva, Z. (2020) Malate–aspartate shuttle promotes l-lactate oxidation in mitochondria. *J. Cell. Physiol.* **235**, 2569–2581
126. Louie, M. C., Ton, J., Brady, M. L., Le, D. T., Mar, J. N., Lerner, C. A., Gerencser, A. A., and Mookerjee, S. A. (2020) Total cellular ATP production changes with primary substrate in MCF7 breast cancer cells. *Front. Oncol.* **10**, 1–12
127. Hill, B. G., Benavides, G. A., Lancaster, J. J. R., Ballinger, S., Dell'Italia, L., Zhang, J., and Darley-Usmar, V. M. (2012) Integration of cellular bioenergetics with mitochondrial quality control and autophagy. *Biol. Chem.* **393**, 1485–1512
128. Zorova, L. D., Popkov, V. A., Plotnikov, E. Y., Silachev, D. N., Pevzner, I. B., Jankauskas, S. S., Babenko, V. A., Zorov, S. D., Balakireva, A. V., Juhaszova, M., Sollott, S. J., and Zorov, D. B. (2018) Mitochondrial membrane potential. *Anal. Biochem.* **552**, 50–59
129. Lefranc, C., Friederich-Persson, M., Braud, L., Palacios-Ramirez, R., Karlsson, S., Boujardine, N., Motterlini, R., Jaisser, F., and Nguyen Dinh Cat, A. (2019) MR (mineralocorticoid receptor) induces adipose tissue senescence and mitochondrial dysfunction leading to vascular dysfunction in obesity. *Hypertension* **73**, 458–468
130. Rojas-Morales, P., León-Contreras, J. C., Aparicio-Trejo, O. E., Reyes-Ocampo, J. G., Medina-Campos, O. N., Jiménez-Osorio, A. S., González-Reyes, S., Marquina-Castillo, B., Hernández-Pando, R., Barrera-Oviedo, D., Sánchez-Lozada, L. G., Pedraza-Chaverri, J., and Tapia, E. (2019) Fasting reduces oxidative stress, mitochondrial dysfunction and fibrosis induced by renal ischemia-reperfusion injury. *Free Radic. Biol. Med.* **135**, 60–67
131. Ehrenberg, B., Montana, V., Wei, M. D., Wuskell, J. P., and Loew, L. M. (1988) Membrane potential can be determined in individual cells from the nernstian distribution of cationic dyes. *Biophys. J.* **53**, 785–794
132. Hoek, J. B., Nicholls, D. G., and Williamson, J. R. (1980) Determination of the mitochondrial protonmotive force in isolated hepatocytes. *J. Biol. Chem.* **255**, 1458–1464
133. Ward, M. W., Rego, A. C., Frenguelli, B. G., and Nicholls, D. G. (2000) Mitochondrial membrane potential and glutamate excitotoxicity in cultured cerebellar granule cells. *J. Neurosci.* **20**, 7208–7219
134. Scaduto, R. C., and Grotyohann, L. W. (1999) Measurement of mitochondrial membrane potential using fluorescent rhodamine derivatives. *Biophys. J.* **76**, 469–477
135. Lemasters, J. J., and Ramshesh, V. K. (2007) Imaging of mitochondrial polarization and depolarization with cationic fluorophores. *Methods Cell Biol.* **80**, 283–295
136. Park, J. S., Davis, R. L., and Sue, C. M. (2018) Mitochondrial dysfunction in Parkinson's disease: New mechanistic insights and therapeutic perspectives. *Curr. Neurol. Neurosci. Rep.* **18**, 21
137. Kelley, D. E., He, J., Menshikova, E. V., and Ritov, V. B. (2002) Dysfunction of mitochondria in human skeletal muscle in type 2 diabetes. *Diabetes* **51**, 2944–2950

138. Romanello, V., Guadagnin, E., Gomes, L., Roder, I., Sandri, C., Petersen, Y., Milan, G., Masiero, E., Del Piccolo, P., Foretz, M., Scorrano, L., Rudolf, R., and Sandri, M. (2010) Mitochondrial fission and remodelling contributes to muscle atrophy. *EMBO J.* **29**, 1774–1785
139. Roden, M., Price, T. B., Perseghin, G., Petersen, K. F., Rothman, D. L., Cline, G. W., and Shulman, G. I. (1996) Mechanism of free fatty acid-induced insulin resistance in humans. *J. Clin. Invest.* **97**, 2859–2865
140. Lowell, B. B., and Shulman, G. I. (2005) Mitochondrial dysfunction and type 2 diabetes. *Curr. Diab. Rep.* **307**, 384–387
141. Petersen, K. F., Befroy, D., Dufour, S., Dziura, J., Ariyan, C., Rothman, D. L., DiPietro, L., Cline, G. W., and Shulman, G. I. (2003) Mitochondrial dysfunction in the elderly: Possible role in insulin resistance. *Science* **300**, 1140–1142
142. Muoio, D. M. (2010) Intramuscular triacylglycerol and insulin resistance: Guilty as charged or wrongly accused? *Biochim. Biophys. Acta* **1801**, 281–288
143. Ghosh, S., Wicks, S. E., Vandanmagsar, B., Mendoza, T. M., Bayless, D. S., Salbaum, J. M., Dearth, S. P., Campagna, S. R., Mynatt, R. L., and Noland, R. C. (2019) Extensive metabolic remodeling after limiting mitochondrial lipid burden is consistent with an improved metabolic health profile. *J. Biol. Chem.* **294**, 12313–12327
144. Bonnard, C., Durand, A., Peyrol, S., Chansaume, E., Chauvin, M. A., Morio, B., Vidal, H., and Rieusset, J. (2008) Mitochondrial dysfunction results from oxidative stress in the skeletal muscle of diet-induced insulin-resistant mice. *J. Clin. Invest.* **118**, 789–800
145. Fisher-Wellman, K. H., Weber, T. M., Cathey, B. L., Brophy, P. M., Gilliam, L. A. A., Kane, C. L., Maples, J. M., Gavin, T. P., Houmard, J. A., and Neuffer, P. D. (2014) Mitochondrial respiratory capacity and content are normal in young insulin-resistant obese humans. *Diabetes* **63**, 132–141
146. Phielix, E., Schrauwen-Hinderling, V. B., Mensink, M., Lenaers, E., Meex, R., Hoeks, J., Kooi, M. E., Moonen-Kornips, E., Sels, J. P., Hesselink, M. K. C., and Schrauwen, P. (2008) Lower intrinsic ADP-stimulated mitochondrial respiration underlies *in vivo* mitochondrial dysfunction in muscle of male type 2 diabetic patients. *Diabetes* **57**, 2943–2949
147. Randle, P. J., Garland, P. B., Hales, C. N., and Newsholme, E. A. (1963) The glucose fatty-acid cycle its role in insulin sensitivity and the metabolic disturbances of diabetes mellitus. *Lancet* **281**, 785–789
148. Denton, R. M., and Randle, P. J. (1966) Citrate and the regulation of adipose-tissue phosphofructokinase. *Biochem. J.* **100**, 420–423
149. Ramakrishna, R., Edwards, J. S., McCulloch, A., and Palsson, B. O. (2001) Flux-balance analysis of mitochondrial energy metabolism: Consequences of systemic stoichiometric constraints. *Am. J. Physiol. Regul. Integr. Comp. Physiol.* **280**, 695–704
150. Savinell, J. M., and Palsson, B. O. (1992) Network analysis of intermediary metabolism using linear optimization. I. Development of mathematical formalism. *J. Theor. Biol.* **154**, 421–454
151. Neuffer, P. D. (2019) Cutting fuel offers new clues in diabetic mystery. *J. Biol. Chem.* **294**, 12328–12329
152. Hancock, C. R., Han, D. H., Chen, M., Terada, S., Yasuda, T., Wright, D. C., and Holloszy, J. O. (2008) High-fat diets cause insulin resistance despite an increase in muscle mitochondria. *Proc. Natl. Acad. Sci. U. S. A.* **105**, 7815–7820
153. Holloszy, J. O. (2013) "Deficiency" of mitochondria in muscle does not cause insulin resistance. *Diabetes* **62**, 1036–1040
154. Leckey, J. J., Hoffman, N. J., Parr, E. B., Devlin, B. L., Trewin, A. J., Stepto, N. K., Morton, J. P., Burke, L. M., and Hawley, J. A. (2018) High dietary fat intake increases fat oxidation and reduces skeletal muscle mitochondrial respiration in trained humans. *FASEB J.* **32**, 2979–2991
155. Murphy, M. P. (2009) How mitochondria produce reactive oxygen species. *Biochem. J.* **417**, 1–13
156. Anderson, E. J., Lustig, M. E., Boyle, K. E., Woodlief, T. L., Kane, D. A., Lin, C.-T., Price, J. W., Kang, L., Rabinovitch, P. S., Szeto, H. H., Houmard, J. A., Cortright, R. N., Wasserman, D. H., and Neuffer, P. D. (2009) Mitochondrial H₂O₂ emission and cellular redox state link excess fat intake to insulin resistance in both rodents and humans. *J. Clin. Invest.* **119**, 573–581
157. Houstis, N., Rosen, E. D., and Lander, E. S. (2006) Reactive oxygen species have a causal role in multiple forms of insulin resistance. *Nature* **440**, 944–948
158. Fazakerley, D. J., Minard, A. Y., Krycer, J. R., Thomas, K. C., Stöckli, J., Harney, D. J., Burchfield, J. G., Maghzal, G. J., Caldwell, S. T., Hartley, R. C., Stocker, R., Murphy, M. P., and James, D. E. (2018) Mitochondrial oxidative stress causes insulin resistance without disrupting oxidative phosphorylation. *J. Biol. Chem.* **293**, 7315–7328
159. Fazakerley, D. J., Chaudhuri, R., Yang, P., Maghzal, G. J., Thomas, K. C., Krycer, J. R., Humphrey, S. J., Parker, B. L., Fisher-Wellman, K. H., Meoli, C. C., Hoffman, N. J., Diskin, C., Burchfield, J. G., Cowley, M. J., Kaplan, W., *et al.* (2018) Mitochondrial CoQ deficiency is a common driver of mitochondrial oxidants and insulin resistance. *Elife* **7**, e32111
160. Hüttemann, M., Lee, I., Pecinova, A., Pecina, P., Przyklenk, K., and Doan, J. W. (2008) Regulation of oxidative phosphorylation, the mitochondrial membrane potential, and their role in human disease. *J. Bioenerg. Biomembr.* **40**, 445–456
161. Guarás, A., Perales-Clemente, E., Calvo, E., Acín-Pérez, R., Loureiro-Lopez, M., Pujol, C., Martínez-Carrascoso, I., Nuñez, E., García-Marqués, F., Rodríguez-Hernández, M. A., Cortés, A., Diaz, F., Pérez-Martos, A., Moraes, C. T., Fernández-Silva, P., *et al.* (2016) The CoQH2/CoQ ratio serves as a sensor of respiratory chain efficiency. *Cell Rep.* **15**, 197–209
162. McLaughlin, K. L., McClung, J. M., and Fisher-Wellman, K. H. (2018) Bioenergetic consequences of compromised mitochondrial DNA repair in the mouse heart. *Biochem. Biophys. Res. Commun.* **504**, 742–748
163. Trifunovic, A., Wredenberg, A., Falkenberg, M., Spelbrink, J. N., Rovio, A. T., Bruder, C. E., Bohlooly-Y, M., Gldlöf, S., Oldfors, A., Wibom, R., Törnell, J., Jacobs, H. T., and Larsson, N. G. (2004) Premature ageing in mice expressing defective mitochondrial DNA polymerase. *Nature* **429**, 417–423
164. Dykens, J. A., Jamieson, J., Marroquin, L., Nadanaciva, S., Billis, P. A., and Will, Y. (2008) Biguanide-induced mitochondrial dysfunction yields increased lactate production and cytotoxicity of aerobically-poised HepG2 cells and human hepatocytes *in vitro*. *Toxicol. Appl. Pharmacol.* **233**, 203–210
165. Pereira, C. V., Nadanaciva, S., Oliveira, P. J., and Will, Y. (2012) The contribution of oxidative stress to drug-induced organ toxicity and its detection *in vitro* and *in vivo*. *Expert Opin. Drug Metab. Toxicol.* **8**, 219–237
166. Ježek, J., Cooper, K. F., and Strich, R. (2018) Reactive oxygen species and mitochondrial dynamics: The yin and yang of mitochondrial dysfunction and cancer progression. *Antioxidants (Basel)* **7**, 13
167. Peoples, J. N., Saraf, A., Ghazal, N., Pham, T. T., and Kwong, J. Q. (2019) Mitochondrial dysfunction and oxidative stress in heart disease. *Exp. Mol. Med.* **51**, 1–13
168. Rocha, M., and Springett, R. (2019) Measuring the functionality of the mitochondrial pumping complexes with multi-wavelength spectroscopy. *Biochim. Biophys. Acta Bioenerg.* **1860**, 89–101
169. Ruas, J. S., Siqueira-Santos, E. S., Amigo, I., Rodrigues-Silva, E., Kowaltowski, A. J., and Castilho, R. F. (2016) Underestimation of the maximal capacity of the mitochondrial electron transport system in oligomycin-treated cells. *PLoS One* **11**, e0150967
170. Dranka, B. P., Hill, B. G., and Darley-Usmar, V. M. (2010) Mitochondrial reserve capacity in endothelial cells: The impact of nitric oxide and reactive oxygen species. *Free Radic. Biol. Med.* **48**, 905–914
171. Tonkonogi, M., and Sahlin, K. (1997) Rate of oxidative phosphorylation in isolated mitochondria from human skeletal muscle: Effect of training status. *Acta Physiol. Scand.* **161**, 345–353
172. Suarez, R. K., Staples, J. F., Lighton, J. R. B., and West, T. G. (1997) Relationships between enzymatic flux capacities and metabolic flux rates: Nonequilibrium reactions in muscle glycolysis. *Proc. Natl. Acad. Sci. U. S. A.* **94**, 7065–7069
173. Connett, R. J. (1988) Analysis of metabolic control: New insights using scaled creatine kinase model. *Am. J. Physiol.* **254**, R949–R959
174. Cairns, C. B., Walther, J., Harken, A. H., and Banerjee, A. (1998) Mitochondrial oxidative phosphorylation thermodynamic efficiencies reflect physiological organ roles. *Am. J. Physiol.* **274**, R1376–R1383

175. Waggoner, A. S. (1979) Dye indicators of membrane potential. *Annu. Rev. Biophys. Bioeng.* **8**, 47–68
176. Nicholls, D. G. (2006) Simultaneous monitoring of ionophore- and inhibitor-mediated plasma and mitochondrial membrane potential changes in cultured neurons. *J. Biol. Chem.* **281**, 14864–14874
177. Krumschnabel, G., Eigentler, A., Fasching, M., and Gnaiger, E. (2014) *Use of Safranin for the Assessment of Mitochondrial Membrane Potential by High-Resolution Respirometry and Fluorometry*, 1st Ed, Elsevier Inc, Amsterdam, The Netherlands
178. Perry, S. W., Norman, J. P., Barbieri, J., Brown, E. B., and Gelbard, H. A. (2011) Mitochondrial membrane potential probes and the proton gradient: A practical usage guide. *Biotechniques* **50**, 98–115
179. Chance, B. (1952) Spectra and reaction kinetics of respiratory pigments of homogenized and intact cells. *Nature* **169**, 215–221
180. Nisr, R. B., and Affourtit, C. (2014) Insulin acutely improves mitochondrial function of rat and human skeletal muscle by increasing coupling efficiency of oxidative phosphorylation. *Biochim. Biophys. Acta* **1837**, 270–276
181. Choi, S. W., Gerencser, A. A., and Nicholls, D. G. (2009) Bioenergetic analysis of isolated cerebrocortical nerve terminals on a microgram scale: Spare respiratory capacity and stochastic mitochondrial failure. *J. Neurochem.* **109**, 1179–1191
182. Nickens, K. P., Wikstrom, J. D., Shirihai, O. S., Patierno, S. R., and Ceryak, S. (2013) A bioenergetic profile of non-transformed fibroblasts uncovers a link between death-resistance and enhanced spare respiratory capacity. *Mitochondrion* **13**, 662–667
183. Malinska, D., Szymański, J., Patalas-Krawczyk, P., Michalska, B., Wojtala, A., Prill, M., Partyka, M., Drabik, K., Walczak, J., Sewer, A., John, S., Luettich, K., Peitsch, M. C., Hoeng, J., Duszyński, J., et al. (2018) Assessment of mitochondrial function following short- and long-term exposure of human bronchial epithelial cells to total particulate matter from a candidate modified-risk tobacco product and reference cigarettes. *Food Chem. Toxicol.* **115**, 1–12
184. Abe, Y., Sakairi, T., Kajiyama, H., Shrivastav, S., Beeson, C., and Kopp, J. B. (2010) Bioenergetic characterization of mouse podocytes. *Am. J. Physiol. Cell Physiol.* **299**, 464–476
185. Selenius, L. A., Lundgren, M. W., Jawad, R., Danielsson, O., and Björnstedt, M. (2019) The cell culture medium affects growth, phenotype expression and the response to selenium cytotoxicity in A549 and HepG2 cells. *Antioxidants* **8**, 130
186. Ježek, J., Plecítá-Hlavatá, L., and Ježek, P. (2018) Aglycemic HepG2 cells switch from aminotransferase glutaminolytic pathway of pyruvate utilization to complete Krebs cycle at hypoxia. *Front. Endocrinol. (Lausanne)* **9**, 1–14
187. Marcinek, D. J., Schenkman, K. A., Ciesielski, W. A., and Conley, K. E. (2004) Mitochondrial coupling *in vivo* in mouse skeletal muscle. *Am. J. Physiol. Cell Physiol.* **286**, 457–463
188. Marcinek, D. J., Schenkman, K. A., Ciesielski, W. A., Lee, D., and Conley, K. E. (2005) Reduced mitochondrial coupling *in vivo* alters cellular energetics in aged mouse skeletal muscle. *J. Physiol.* **569**, 467–473
189. Siegel, M. P., Kruse, S. E., Knowels, G., Salmon, A., Beyer, R., Xie, H., van Remmen, H., Smith, S. R., and Marcinek, D. J. (2011) Reduced coupling of oxidative phosphorylation *in vivo* precedes electron transport chain defects due to mild oxidative stress in mice. *PLoS One* **6**, e26963
190. To, T. L., Cuadros, A. M., Shah, H., Hung, W. H. W., Li, Y., Kim, S. H., Rubin, D. H. F., Boe, R. H., Rath, S., Eaton, J. K., Piccioni, F., Goodale, A., Kalani, Z., Doench, J. G., Root, D. E., et al. (2019) A compendium of genetic modifiers of mitochondrial dysfunction reveals intra-organelle buffering. *Cell* **179**, 1222–1238.e17
191. Sullivan, L. B., Gui, D. Y., Hosios, A. M., Bush, L. N., Freinkman, E., and Vander Heiden, M. G. (2015) Supporting aspartate biosynthesis is an essential function of respiration in proliferating cells. *Cell* **162**, 552–563
192. Brookes, P. S., Rolfe, D. F. S., and Brand, M. D. (1997) The proton permeability of liposomes made from mitochondrial inner membrane phospholipids: Comparison with isolated mitochondria. *J. Membr. Biol.* **155**, 167–174
193. Ježek, P., Jabůrek, M., and Porter, R. K. (2019) Uncoupling mechanism and redox regulation of mitochondrial uncoupling protein 1 (UCP1). *Biochim. Biophys. Acta Bioenerg.* **1860**, 259–269
194. Ricquier, D., and Kader, J. C. (1976) Mitochondrial protein alteration in active brown fat: A sodium dodecyl sulfate-polyacrylamide gel electrophoretic study. *Biochem. Biophys. Res. Commun.* **73**, 577–583
195. Bertholet, A. M., Chouchani, E. T., Kazak, L., Angelin, A., Fedorenko, A., Long, J. Z., Vidoni, S., Garrity, R., Cho, J., Terada, N., Wallace, D. C., Spiegelman, B. M., and Kirichok, Y. (2019) H⁺ transport is an integral function of the mitochondrial ADP/ATP carrier. *Nature* **571**, 515–520
196. Samartsev, V. N., Smirnov, A. V., Zeldi, I. P., Markova, O. V., Mokhova, E. N., and Skulachev, V. P. (1997) Involvement of aspartate/glutamate antiporter in fatty acid-induced uncoupling of liver mitochondria. *Biochim. Biophys. Acta* **1319**, 251–257
197. Vozza, A., Parisi, G., De Leonardi, F., Lasorsa, F. M., Castegna, A., Amorese, D., Marmo, R., Calcagnile, V. M., Palmieri, L., Ricquier, D., Paradies, E., Scarcia, P., Palmieri, F., Bouillaud, F., and Fiermonte, G. (2014) UCP2 transports C4 metabolites out of mitochondria, regulating glucose and glutamine oxidation. *Proc. Natl. Acad. Sci. U. S. A.* **111**, 960–965
198. Bouillaud, F., Alves-Guerra, M. C., and Ricquier, D. (2016) UCPs, at the interface between bioenergetics and metabolism. *Biochim. Biophys. Acta* **1863**, 2443–2456
199. Starkov, A. A., Dedukhova, V. I., and Skulachev, V. P. (1994) 6-Ketocholesterol abolishes the effect of the most potent uncouplers of oxidative phosphorylation in mitochondria. *FEBS Lett.* **355**, 305–308
200. Owen, O. E., Kalhan, S. C., and Hanson, R. W. (2002) The key role of anaplerosis and cataplerosis for citric acid cycle function. *J. Biol. Chem.* **277**, 30409–30412
201. Hakimi, P., Johnson, M. T., Yang, J., Lepage, D. F., Conlon, R. A., Kalhan, S. C., Reshef, L., Tilghman, S. M., and Hanson, R. W. (2005) Phosphoenolpyruvate carboxykinase and the critical role of cataplerosis in the control of hepatic metabolism. *Nutr. Metab.* **2**, 1–12
202. Bernardi, P. (1999) Mitochondrial transport of cations: Channels, exchangers, and permeability transition. *Physiol. Rev.* **79**, 1127–1155
203. Chacinska, A., Koehler, C. M., Milenkovic, D., Lithgow, T., and Pfanner, N. (2009) Importing mitochondrial proteins: Machineries and mechanisms. *Cell* **138**, 628–644
204. Smith, C. D., Schmidt, C. A., Lin, C.-T., Fisher-Wellman, K. H., and Neuffer, P. D. (2020) Flux through mitochondrial redox circuits linked to nicotinamide nucleotide transhydrogenase generates counterbalance changes in energy expenditure. *J. Biol. Chem.* **295**, 16207–16216
205. McLaughlin, K. L., Kew, K. A., McClung, J. M., and Fisher-Wellman, K. H. (2020) Subcellular proteomics combined with bioenergetic phenotyping reveals protein biomarkers of respiratory insufficiency in the setting of proofreading-deficient mitochondrial polymerase. *Sci. Rep.* **10**, 1–10
206. Maxfield, F. R. (1982) Weak bases and ionophores rapidly and reversibly raise the pH of endocytic vesicles in cultured mouse fibroblasts. *J. Cell Biol.* **95**, 676–681
207. Al-Shaikhal, M. H. M., Nedergaard, J., and Cannon, B. (1979) Sodium-induced calcium release from mitochondria in brown adipose tissue. *Proc. Natl. Acad. Sci. U. S. A.* **76**, 2350–2353
208. Souza, A. C., Machado, F. S., Celes, M. R. N., Faria, G., Rocha, L. B., Silva, J. S., and Rossi, M. A. (2005) Mitochondrial damage as an early event of monensin-induced cell injury in cultured fibroblasts L929. *J. Vet. Med. A Physiol. Pathol. Clin. Med.* **52**, 230–237
209. Erecinska, M., Dagan, F., Nelson, D., Deas, J., and Silver, I. A. (1991) Relations between intracellular ions and energy metabolism: A study with monensin in synaptosomes, neurons, and C6 glioma cells. *J. Neurosci.* **11**, 2410–2421
210. Mitchell, P. (1977) Vectorial chemiosmotic processes. *Annu. Rev. Biochem.* **46**, 996–1005
211. Mitchell, P., and Moyle, J. (1969) Estimation of membrane potential and pH difference across the cristae membrane of rat liver mitochondria. *Eur. J. Biochem.* **7**, 471–484
212. Willis, W. T., Jackman, M. R., Messer, J. I., Kuzmiak-Glancy, S., and Glancy, B. (2016) A simple hydraulic analog model of oxidative phosphorylation. *Med. Sci. Sports Exerc.* **48**, 990–1000
213. Fisher-Wellman, K. H., and Neuffer, P. D. (2012) Linking mitochondrial bioenergetics to insulin resistance via redox biology. *Trends Endocrinol. Metab.* **23**, 142–153

JBC REVIEWS: "From OCR and ECAR to energy"

214. Neuffer, P. D. (2018) The bioenergetics of exercise. *Cold Spring Harb. Perspect. Med.* **8**, 1–12
215. Hirst, J. (2013) Mitochondrial complex I. *Annu. Rev. Biochem.* **82**, 551–575
216. Brand, M. (2005) The efficiency and plasticity of mitochondrial energy transduction. *Biochem. Soc. Trans.* **33**, 897–904
217. Hollis, V. S., Palacios-Callender, M., Springett, R. J., Delpy, D. T., and Moncada, S. (2003) Monitoring cytochrome redox changes in the mitochondria of intact cells using multi-wavelength visible light spectroscopy. *Biochim. Biophys. Acta* **1607**, 191–202
218. Soga, N., Kimura, K., Kinoshita, K., Yoshida, M., and Suzuki, T. (2017) Perfect chemomechanical coupling of FoF1-ATP synthase. *Proc. Natl. Acad. Sci. U. S. A.* **114**, 4960–4965
219. Schendzielorz, A. B., Schulz, C., Lytovchenko, O., Clancy, A., Guiard, B., Ieva, R., van der Laan, M., and Rehling, P. (2017) Two distinct membrane potential-dependent steps drive mitochondrial matrix protein translocation. *J. Cell Biol.* **216**, 83–92
220. Jonckheere, A. I., Smeitink, J. A. M., and Rodenburg, R. J. T. (2012) Mitochondrial ATP synthase: Architecture, function and pathology. *J. Inherit. Metab. Dis.* **35**, 211–225
221. Hoek, J. B., and Rydstrom, J. (1988) Physiological roles of nicotinamide nucleotide transhydrogenase. *Biochem. J.* **254**, 1–10
222. Berry, B. J., Trewin, A. J., Amitrano, A. M., Kim, M., and Wojtovich, A. P. (2018) Use the protonmotive force: Mitochondrial uncoupling and reactive oxygen species. *J. Mol. Biol.* **430**, 3873–3891
223. Klingenberg, M. (2008) The ADP and ATP transport in mitochondria and its carrier. *Biochim. Biophys. Acta* **1778**, 1978–2021
224. Anandakrishnan, R., Zhang, Z., Donovan-Maiye, R., and Zuckerman, D. M. (2016) Biophysical comparison of ATP synthesis mechanisms shows a kinetic advantage for the rotary process. *Proc. Natl. Acad. Sci. U. S. A.* **113**, 11220–11225
225. Hafner, R. P., and Brand, M. D. (1991) Effect of protonmotive force on the relative proton stoichiometries of the mitochondrial proton pumps. *Biochem. J.* **275**, 75–80